Novel Radioiodinated Aurones as Probes for SPECT Imaging of β-Amyloid Plaques in the Brain

Yoshifumi Maya,[†] Masahiro Ono,*[,†,‡] Hiroyuki Watanabe,[†] Mamoru Haratake,[†] Hideo Saji,[‡] and Morio Nakayama*[,†]

Department of Hygienic Chemistry, Graduate School of Biomedical Sciences, Nagasaki University, 1-14 Bunkyo-machi, Nagasaki 852-8521, and Department of Patho-Functional Bioanalysis, Graduate School of Pharmaceutical Sciences, Kyoto University, 46−29 Yoshida Shimoadachi-cho, Sakyo-ku, Kyoto 606-8501, Japan. Received July 29, 2008; Revised Manuscript Received November 10, 2008

We report a novel series of radioiodinated aurone derivatives as probes for imaging Aβ plaques in the brains of patients with Alzheimer's disease (AD) using single photon emission computed tomography (SPECT). In binding experiments in vitro, aurone derivatives showed very good affinity for Aβ aggregates (K_i = 1.1 to 3.4 nM). No-carrier-added radioiodinated aurones were successfully prepared through an iododestannylation reaction from the corresponding tributyltin derivatives. In biodistribution experiments using normal mice, aurone derivatives displayed high brain uptake (1.7−4.5% ID/g at 2 min) and rapid clearance from the brain (0.1−0.4% ID/g at 30 min), especially [^{125}I]**15**. Furthermore, a specific plaque labeling signal was observed in in vitro autoradiography of postmortem AD brain sections using [^{125}I]**15**. [^{125}I]**15** may be a useful SPECT imaging agent for detecting Aβ plaques in the brain of AD.

INTRODUCTION

Alzheimer's disease (AD) is a progressive neurodegenerative disorder characterized by cognitive decline, irreversible memory loss, disorientation, and language impairment. Senile plaques containing β-amyloid (Aβ) peptides and neurofibrillary tangles in the postmortem brain are two pathological hallmarks of AD (*1, 2*). Excessive production of Aβ via various normal or abnormal mechanisms is considered to be the initial neurodegenerative event in AD. Currently, it is difficult for clinicians to differentiate between the cognitive decline associated with normal aging and the cognitive decline associated with AD. There is no simple and definitive diagnostic method to detect Aβ plaques in the brain without postmortem pathological staining of brain tissue. Thus, the development of imaging agents for positron emission tomography (PET) or single photon emission computed tomography (SPECT), which can detect Aβ plaques in vivo, may assist with the early diagnosis of AD (*3−5*).

In the past few years, several groups have reported potential amyloid-imaging probes for the detection of Aβ plaques in vivo. Tracers such as [^{11}C]PIB (*6, 7*), [^{11}C]SB-13 (*8, 9*), [^{18}F]BAY94-9172 (*10*), [^{11}C]BF-227 (*11*), [^{18}F]FDDNP (*12−14*), and [^{123}I]IMPY (*15−18*) have been tested clinically and demonstrated utility (Figure 1). [^{123}I]IMPY is the only tracer for SPECT; the other five tracers are amyloid imaging probes for PET. Since SPECT is more valuable than PET in terms of routine diagnostic use, the development of more useful β-amyloid-imaging agents for SPECT has been a critical issue.

Recently, we have reported that radioiodinated aurones possessing a nucleophilic group (NH_2, NHMe, and NMe_2) function as a new backbone structure in the development of amyloid-imaging probes for SPECT (*19*). These compounds showed strong binding to Aβ aggregates (K_i = 1.2−6.8 nM), good penetration of the brain (1.9−4.6% ID/g at 2 min), and a fast washout from the brain (0.3−0.5% ID/g at 30 min). However, the aurone derivatives appeared inferior to IMPY in pharmacokinetics, although their high affinity for β-amyloid plaques is sufficient for imaging in vivo. Therefore, additional structural changes are essential to further improve the properties of aurone derivatives to make them suitable for the imaging of β-amyloid plaques in the brain.

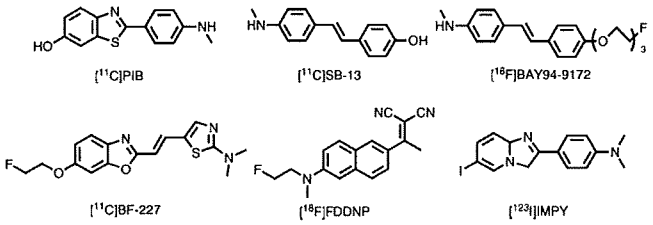

Figure 1. Chemical structure of Aβ imaging probes clinically tested.

To develop more promising aurones for SPECT-based imaging of β-amyloid plaques, we designed a novel series of radioiodinated derivatives with poly(ethylene glycol) (PEG). PEG is nontoxic, nonimmunogenic, highly soluble in water, and FDA-approved, and PEGylation has been used to change the pharmacokinetics of various biologically interesting proteins or peptides, leading to better therapeutics (*20, 21*). Therefore, PEGylated aurone derivatives are worthy of further evaluation as novel β-amyloid-imaging probes for SPECT.

In the present study, we designed and synthesized a novel series of radioiodinated aurone derivatives with not only 1 to 3 units of ethylene glycol at the 4′ position, but also other nucleophilic groups (-OCH_3 and -OH), and evaluated their biological potential as probes for imaging β-amyloid by testing their affinity for Aβ aggregates in vitro and their uptake by and

* To whom correspondence should be addressed. Phone +81-75-753-4608, Fax +81-75-753-4568, e-mail ono@pharm.kyoto-u.ac.jp for M. Ono. Phone +81-95-819-2441, Fax +81-95-819-2441, e-mail morio@nagasaki-u.ac.jp for M. Nakayama.
[†] Nagasaki University.
[‡] Kyoto University.

10.1021/bc8003292 CCC: $40.75
Published on Web 12/11/2008

clearance from the brain in biodistribution experiments using normal mice.

MATERIALS AND METHODS

All reagents were commercial products and used without further purification unless otherwise indicated. ^{1}H NMR spectra were obtained on a Varian Gemini 300 spectrometer with TMS as an internal standard. Coupling constants are reported in hertz. Multiplicity was defined by s (singlet), d (doublet), t (triplet), and m (multiplet). Mass spectra were obtained on a JEOL IMS-DX instrument.

Chemistry. *Methyl 2-((Ethoxycarbonyl)methoxy)-5-bromobenzoate* (**1**). To a solution of 2-hydroxy-5-bromobenzoic acid methyl ester (1.5 g, 6.49 mmol) in acetone (10 mL) was added K_2CO_3 (2.7 g, 19.5 mmol) and ethylbromoacetate (1.3 mL, 7.78 mmol). The mixture was stirred for 3 h under reflux. After the solvent was evaporated, the residue was dissolved in water (100 mL) and extracted with ethyl acetate (100 mL). The organic layer was dried over Na_2SO_4, and evaporation of the solvent gave 1.60 g of **1** (77.7%). ^{1}H NMR NMR (300 MHz, $CDCl_3$) δ 1.29 (t, J = 7.2 Hz, 3H), 3.91 (s, 3H), 4.24 (q, J = 7.2 Hz, 2H), 4.69 (s, 2H), 6.78 (d, J = 9.0 Hz, 1H), 7.54 (d, J = 6.3 Hz, 1H), 7.96 (s, 1H).

2-(Carboxymethoxy)-5-bromobenzoic Acid (**2**). To a solution of **1** (1.6 g, 5.04 mmol) in methanol (10 mL) was added 10% aqueous KOH (3.0 mL). The mixture was stirred for 2 h at room temperature. The product formed by adding 1 N HCl was filtered to give 1.10 g of **2** (79.4%). ^{1}H NMR (300 MHz, CD_3OD) δ 4.81 (s, 2H), 7.02 (d, J = 8.7 Hz, 1H), 7.63 (dd, J = 2.4, 2.7 Hz, 1H), 7.93 (d, J = 2.4 Hz, 1H).

5-Bromo-3-acetoxybenzofuran (**3**). A mixture of acetic anhydride (20 mL), acetic acid (4 mL), anhydrous sodium acetate (1.0 g, 12.0 mmol), and **2** (100 mg, 0.36 mmol) was heated to reflux for 5 h. Water (100 mL) was then added, and the mixture was extracted with chloroform (100 mL). After drying of the organic layer on Na_2SO_4, evaporation gave 78 mg of **3** (86.5%). ^{1}H NMR (300 MHz, $CDCl_3$) δ 2.37 (s, 3H), 7.33 (d, J = 9.0 Hz, 1H), 7.43 (dd, J = 3.6, 2.1 Hz, 1H), 7.71 (s, 1H), 8.02 (s, 1H).

5-Bromobenzofuran-3(2H)-one (**4**). A mixture of **3** (78 mg, 0.31 mmol), methanol (3 mL), water (1 mL), and 1 N HCl (2 mL) was heated to reflux for 3 h. The precipitate formed was collected by filtration, washed with water, and dried under vacuum to obtain 15 mg of **4** (22.5%). ^{1}H NMR (300 MHz, $CDCl_3$) δ 4.67 (s, 2H), 7.06 (d, J = 9.0 Hz, 1H), 7.69 (dd, J = 2.1, 2.1 Hz, 1H), 7.79 (d, J = 2.1 Hz, 1H).

(Z)-2-(4-Methoxybenzylidene)-5-bromobenzofuran-3(2H)-one (**5**). To a solution of **4** (300 mg, 1.41 mmol) and 4-methoxybenzaldehyde (192 mg, 1.41 mmol) in chloroform (5 mL) was added Al_2O_3 (2.7 g, 26.0 mmol). The mixture was stirred for 20 min at room temperature. After filtration of the reaction mixture, the solvent of the filtrate was removed, and drying under vacuum yielded 410 mg of **5** (85.7%). ^{1}H NMR (300 MHz, $CDCl_3$) δ 3.88 (s, 3H), 6.91 (s, 1H), 6.99 (d, J = 9.0 Hz, 2H), 7.24 (d, J = 8.4 Hz, 1H), 7.73 (dd, J = 2.1, 2.1 Hz, 1H), 7.88 (d, J = 8.7 Hz, 2H), 7.92 (d, J = 1.8 Hz, 1H).

(Z)-2-(4-Hydroxybenzylidene)-5-bromobenzofuran-3(2H)-one (**6**). BBr_3 (3 mL, 1 M solution in CH_2Cl_2) was added to a solution of **5** (300 mg, 0.91 mmol) in CH_2Cl_2 (25 mL) dropwise in an ice bath. The mixture was allowed to warm to room temperature and stirred for 15 h. Water (50 mL) was added while the reaction mixture was cooled in an ice bath. The mixture was extracted with chloroform (2 × 30 mL), and the organic phase was dried over Na_2SO_4 and filtered. The filtrate was concentrated and the residue was purified by silica gel chromatography (hexane/ethyl acetate = 2:3) to give 15 mg of **6** (5.2%). ^{1}H NMR (300 MHz, DMSO-d_6) δ 1.23 (s, 1H), 6.92 (d, J = 8.4 Hz, 2H), 6.96 (s, 1H), 7.56 (d, J = 9.3 Hz, 1H), 7.88−7.92 (m, 3H), 7.95 (s, 1H). MS (EI) m/z 316 [M^+].

(Z)-2-(4-Methoxybenzylidene)-5-(tributylstannyl)benzofuran-3(2H)-one (**7**). A mixture of **5** (200 mg, 0.60 mmol), $(Bu_3Sn)_2$ (0.4 mL), and $(Ph_3P)_4Pd$ (50 mg, 0.043 mmol) in a mixed solvent (15 mL, 1:1 dioxane/Et_3N) was stirred under reflux for 24 h. The solvent was removed, and the resulting residue was purified by silica gel chromatography using chloroform to give 50 mg of **7** (15.3%). ^{1}H NMR (300 MHz, $CDCl_3$) δ 0.89−1.64 (m, 27H), 3.87 (s, 3H), 6.89 (s, 1H), 6.99 (d, J = 8.7 Hz, 2H), 7.31 (d, J = 8.1 Hz, 1H), 7.71 (dd, J = 0.9, 0.9 Hz, 1H), 7.86 (d, J = 9.0 Hz, 2H), 7.90 (d, J = 8.7 Hz 1H). MS (EI) m/z 528 [M^+].

(Z)-2-(4-Hydroxybenzylidene)-5-(tributylstannyl)benzofuran-3(2H)-one (**8**). The same reaction as described above to prepare **7** was used, and 10 mg of **8** was obtained in a 12.0% yield from **6**. ^{1}H NMR (300 MHz, $CDCl_3$) δ 0.86−1.60 (m, 27H), 6.74 (d, J = 9.0 Hz, 2H), 6.90 (s, 1H), 7.30 (d, J = 8.1 Hz, 1H), 7.69 (d, J = 8.1 Hz, 1H), 7.80 (d, J = 8.4 Hz, 2H), 7.89 (s, 1H). MS (EI) m/z 542 [M^+].

(Z)-2-(4-Methoxybenzylidene)-5-iodobenzofuran-3(2H)-one (**9**). To a solution of **7** (10 mg, 0.03 mmol) in $CHCl_3$ (3 mL) was added a solution of iodine in $CHCl_3$ (1 mL, 0.25 M) at room temperature. The mixture was stirred at room temperature for 5 min, and saturated $NaHSO_3$ solution (15 mL) was added. The organic phase was separated, dried over Na_2SO_4, and filtered. The solvent was removed, and the residue was purified by preparative TLC (2:3 hexane/ethyl acetate) to give 6 mg of **9** (84.0%). ^{1}H NMR (300 MHz, $CDCl_3$) δ 3.88 (s, 3H), 6.91 (s, 1H), 6.98 (d, J = 6.9 Hz, 2H), 7.14 (d, J = 8.4 Hz, 1H), 7.87−7.91 (m, 3H), 8.12 (d, J = 2.1 Hz, 1H). HRMS (EI) m/z calcd for $C_{16}H_{11}O_3I$ (M^+) 377.9753, found 377.9753.

Methyl 2-((Ethoxycarbonyl)methoxy)-5-iodobenzoate (**10**). The same reaction as described above to prepare **1** was used, and 2.62 g of **10** was obtained in a 99.0% yield from 2-hydroxy-5-iodobenzoic acid methyl ester. ^{1}H NMR (300 MHz, $CDCl_3$) δ 1.29 (t, J = 7.2 Hz, 3H), 3.90 (s, 3H), 4.25 (q, J = 6.0 Hz, 2H), 4.69 (s, 2H), 6.66 (d, J = 8.7 Hz, 1H), 7.71 (dd, J = 2.4, 2.4 Hz, 1H), 8.12 (d, J = 2.1 Hz, 1H).

2-(Carboxymethoxy)-5-iodobenzoic Acid (**11**). The same reaction as described above to prepare **2** was used, and 2.02 g of **11** was obtained in a 87.2% yield from **10**. ^{1}H NMR (300 MHz, CD_3OD) δ 4.81 (s, 2H), 6.89 (d, J = 9.0 Hz, 1H), 7.80 (dd, J = 2.7, 2.4 Hz, 1H), 8.10 (d, J = 2.4 Hz, 1H).

5-Iodo-3-acetoxybenzofuran (**12**). The same reaction as described above to prepare **3** was used, and 1.45 g of **12** was obtained in a 76.6% yield from **11**. ^{1}H NMR (300 MHz, $CDCl_3$) δ 2.37 (s, 3H), 7.23 (d, J = 8.1 Hz, 1H), 7.59 (dd, J = 1.5, 1.8 Hz, 1H), 7.90 (d, J = 1.5 Hz, 1H), 7.98 (s, 1H).

5-Iodobenzofuran-3(2H)-one (**13**). The same reaction as described above to prepare **4** was used, and 1.17 g of **13** was obtained in a 93.8% yield from **12**. ^{1}H NMR (300 MHz, $CDCl_3$) δ 4.65 (s, 2H), 6.96 (d, J = 9.0 Hz, 1H), 7.85 (dd, J = 1.8, 1.8 Hz, 1H), 7.99 (d, J = 1.8 Hz, 1H).

(Z)-2-(4-Hydroxybenzylidene)-5-iodobenzofuran-3(2H)-one (**14**). The same reaction as described above to prepare **5** was used, and 78 mg of **14** was obtained in a 87.0% yield from **13** and 4-hydroxybenzaldehyde. ^{1}H NMR (300 MHz, $CDCl_3$) δ 1.28 (s, 1H), 6.87 (s, 1H), 6.91 (d, J = 5.4 Hz, 2H), 7.29 (d, J = 8.7 Hz, 1H), 7.85 (d, J = 6.9 Hz, 2H), 8.12 (d, J = 6.9 Hz, 1H), 8.08 (d, J = 1.8 Hz, 1H). HRMS (EI) m/z calcd for $C_{15}H_9O_3I$ (M^+) 363.9596, found 363.9571.

(Z)-2-(4-(2-Hydroxyethoxy)benzylidene)-5-iodobenzofuran-3(2H)-one (**15**). A mixture of potassium carbonate (3.7 g, 26.8 mmol), **14** (194 mg, 0.53 mmol), and ethylene chlorohydrin (0.1 mL, 1.43 mmol) in anhydrous DMF (7 mL) was heated at 120 °C for 15 h. After cooling to room temperature, water was added,

and the reaction mixture was extracted with ethyl acetate. The organic layer was separated, dried over Na_2SO_4, and evaporated. The resulting residue was purified by silica gel chromatography using ethyl acetate to give 123 mg of **15** (56.5%). ^{1}H NMR (300 MHz, $CDCl_3$) δ 2.01 (s, 1H), 4.02 (s, 2H), 4.18 (t, J = 3.9 Hz, 2H), 6.89 (s, 1H), 7.00 (d, J = 7.5 Hz, 2H), 7.14 (d, J = 8.4 Hz, 1H), 7.80−7.92 (m, 3H), 8.12 (d, J = 1.8 Hz, 1H). HRMS (EI) *m/z* calcd for $C_{17}H_{13}O_4I$ (M^+) 407.9859, found 407.9879.

*(Z)-2-(4-(2-(2-Hydroxyethoxy)ethoxy)benzylidene)-5-iodobenzofuran-3(2H)-one (**16**).* The same reaction as described above to prepare **15** was used, and 56 mg of **16** was obtained in a 30.2% yield from **14** and ethylene glycol mono-2-chloroethyl ether. ^{1}H NMR (300 MHz, $CDCl_3$) δ 2.17 (s, 1H), 3.70 (d, J = 4.8 Hz, 2H), 3.78 (d, J = 4.8 Hz, 2H), 3.92 (t, J = 4.8 Hz, 2H), 4.21 (t, J = 4.5 Hz, 2H), 6.89 (s, 1H), 7.00 (d, J = 11.4 Hz, 2H), 7.13 (d, J = 8.7 Hz, 1H), 7.84−7.91 (m, 3H), 8.11 (d, J = 2.1 Hz, 1H). HRMS (EI) *m/z* calcd for $C_{19}H_{17}O_5I$ (M^+) 452.0121, found 452.0131.

*(Z)-2-(4-(2-(2-(2-Hydroxyethoxy)ethoxy)ethoxy)benzylidene)-5-iodobenzofuran-3(2H)-one (**17**).* The same reaction as described above to prepare **15** was used, and 140 mg of **17** was obtained in a 67.9% yield from **14** and 2-[2-(2-chloroethoxy)ethoxy] ethanol. ^{1}H NMR (300 MHz, $CDCl_3$) δ 1.96 (s, 1H), 3.74−3.80 (m, 6H), 3.92 (t, J = 4.8 Hz, 2H), 4.24 (t, J = 4.8 Hz, 2H), 4.45 (t, J = 4.5 Hz, 1H), 4.65 (t, J = 4.5 Hz, 1H), 6.91 (s, 1H), 6.98 (d, J = 9.0 Hz, 2H), 7.15 (d, J = 8.7 Hz, 1H), 7.85−7.92 (m, 3H), 8.15 (d, J = 2.1 Hz, 1H). HRMS (EI) *m/z* calcd for $C_{21}H_{21}O_6I$ (M^+) 496.0383, found 496.0381.

*(Z)-2-(4-(2-Hydroxyethoxy)benzylidene)-5-(tributylstannyl)benzofuran-3(2H)-one (**18**).* The same reaction as described above to prepare **7** was used, and 7 mg of **18** was obtained in a 25.0% yield from **15**. ^{1}H NMR (300 MHz, $CDCl_3$) δ 0.86−1.61 (m, 27H), 2.06 (s, 1H), 4.02 (s, 2H), 4.16 (t, J = 3.6 Hz, 2H), 6.88 (s, 1H), 6.99 (d, J = 9.0 Hz, 2H), 7.30 (d, J = 12.3 Hz, 1H), 7.73 (d, J = 9.0 Hz, 1H), 7.90−7.92 (m, 3H). MS (EI) *m/z* 572 [M^+].

*(Z)-2-(4-(2-(2-Hydroxyethoxy)ethoxy)benzylidene)-5-(tributylstannyl)benzofuran-3(2H)-one (**19**).* The same reaction as described above to prepare **7** was used, and 17 mg of **19** was obtained in a 31.4% yield from **16**. ^{1}H NMR (300 MHz, $CDCl_3$) δ 0.86−1.32 (m, 27H), 2.11 (s, 1H), 3.70 (t, J = 4.8 Hz, 2H), 3.78 (t, J = 4.8 Hz, 2H), 3.91 (t, J = 4.5 Hz, 2H), 4.22 (t, J = 5.1 Hz, 2H), 6.89 (s, 1H), 7.00 (d, J = 7.2 Hz, 2H), 7.31 (d, J = 8.1 Hz, 1H), 7.71 (d, J = 9.0 Hz, 1H), 7.88−7.91 (m, 3H). MS (EI) *m/z* 616 [M^+].

*(Z)-2-(4-(2-(2-(2-Hydroxyethoxy)ethoxy)ethoxy)benzylidene)-5-(tributylstannyl)benzofuran-3(2H)-one (**20**).* The same reaction as described above to prepare **7** was used, and 4 mg of **20** was obtained in a 30.3% yield from **17**. ^{1}H NMR (300 MHz, $CDCl_3$) δ 0.86−1.59 (m, 27H), 2.11 (s, 1H), 3.63 (t, J = 3.3 Hz, 2H), 3.73−3.75 (m, 4H), 3.90 (t, J = 4.2 Hz, 2H), 4.21 (t, J = 4.2 Hz, 2H), 6.88 (s, 1H), 7.10 (d, J = 8.7 Hz, 2H), 7.31 (d, J = 8.1 Hz, 1H), 7.64−7.70 (m, 3H), 7.90 (d, J = 4.8 Hz, 1H). MS (EI) *m/z* 659 [M^+].

Iododestannylation Reaction. The radioiodinated forms of compounds **9**, **14**, **15**, **16**, and **17** were prepared from the corresponding tributyltin derivatives by iododestannylation. Briefly, to initiate the reaction, the tributyltin derivative (50 μg/50 μL EtOH) was added to a mixture of a [^{125}I]NaI (3.7−7.4 MBq, specific activity 2200 Ci/mmol), 50 μL of H_2O_2 (3%), and 50 μL of 1 N HCl in a sealed vial. The reaction was allowed to proceed at room temperature for 2 min and was terminated by addition of $NaHSO_3$. The reaction, after neutralization with sodium bicarbonate, was extracted with ethyl acetate. The extract was dried by passing through an anhydrous Na_2SO_4 column and was then blown dry with a stream of nitrogen gas. The radioiodinated ligand was purified by HPLC on a Cosmosil C_{18} column with an isocratic solvent of H_2O/acetonitrile (3:7) at a flow rate of 1.0 mL/min.

Binding Assays Using the Aggregated Aβ Peptide in Solution. A solid form of Aβ(1−42) was purchased from Peptide Institute (Osaka, Japan). Aggregation was carried out by gently dissolving the peptide (0.25 mg/mL) in a buffer solution (pH 7.4) containing 10 mM sodium phosphate and 1 mM EDTA. The solution was incubated at 37 °C for 42 h with gentle and constant shaking. (*Z*)-2-(4-Aminobenzylidene)-5-iodobenzofuran-3(2*H*)-one ([^{125}I]AAU) was synthesized and used as the radioligand for the competition binding experiments (K_d value of [^{125}I]AAU is 4.2 nM) (*19*). The binding experiments were carried out in 12 × 75 mm borosilicate glass tubes according to a procedure described previously (*19*). A mixture containing 50 μL of test compound (0.8 nM−12.5 μM in 10% ethanol), 50 μL of 0.02 nM [^{125}I]AAU, 50 μL of Aβ(1−42) aggregate, and 850 μL of 10% ethanol was incubated at room temperature for 3 h. The mixture was then filtered through Whatman GF/B filters using a Brandel M-24 cell harvester, and the filters containing the bound ^{125}I ligand were placed in a gamma counter. Values for the half-maximal inhibitory concentration (IC_{50}) were determined from displacement curves of three independent experiments using GraphPad *Prism* 4.0, and those for the inhibition constant (K_i) were calculated using the Cheng-Prusoff equation (*22*): $K_i = IC_{50}/(1 + [L]/K_d)$, where [L] is the concentration of [^{125}I]AAU used in the assay, and K_d is the dissociation constant of AAU (4.2 nM) (*19*).

Staining of Amyloid Plaques in Transgenic Mouse Brain Sections. Tg2576 transgenic mice (20 month of age) were used as an Alzheimer's model. The brain was removed and sliced into serial sections 10 μm thick. Each slide was incubated with a 50% ethanol solution of compound **9**, **14**, **15**, **16**, and **17** (100 μM). Finally, the sections were washed in 50% EtOH for 3 min two times. Fluorescent observation was performed with the Nikon system (Excitation filter, 450−490 nm; Dichroic mirror, DM505; Barrier filter, BA520). Thereafter, the serial sections were also stained with thioflavin S, a pathological dye commonly used for staining Aβ plaques in the brain.

In Vivo Biodistribution in Normal Mice. Animal studies were conducted in accordance with our institutional guidelines and were approved by Nagasaki University Animal Care Committee. A saline solution (100 μL) containing radiolabeled agents (4.2−6.3 kBq) and 10% ethanol was intravenously injected directly into the tail vein of ddY mice (5 weeks old, average weight 20−25 g). The mice were sacrificed at various time points postinjection. The organs of interest were removed and weighed, and the radioactivity was measured with an automatic gamma counter (Aloka, ARC-380). Percent dose per gram of samples was calculated by comparing the sample counts with the counts of the initial dose.

In Vitro Autoradiography. Postmortem brain tissues from an autopsy-confirmed case of AD (73-year-old male) and a control subject (36-year-old male) were obtained from BioChain Institute Inc. The presence and localization of plaques on the sections were confirmed with immunohistochemical staining using a monoclonal Aβ antibody BC05 (Wako) as reported (*23*). The sections were incubated with [^{125}I]**15** (120000 cpm/100 μL) for 1 h at room temperature. They were then dipped in saturated lithium carbonate in 40% EtOH (two 2-min washes) and washed with 40% EtOH (one 2-min wash), before being rinsed with water for 30 s. After drying, the ^{125}I-labeled sections were exposed to a Fuji Film imaging plate overnight.

RESULTS AND DISCUSSION

Chemistry. The target aurone derivatives (**9**, **14**, **15**, **16**, and **17**) were prepared as shown in Schemes 1−3. The synthesis of

Scheme 1

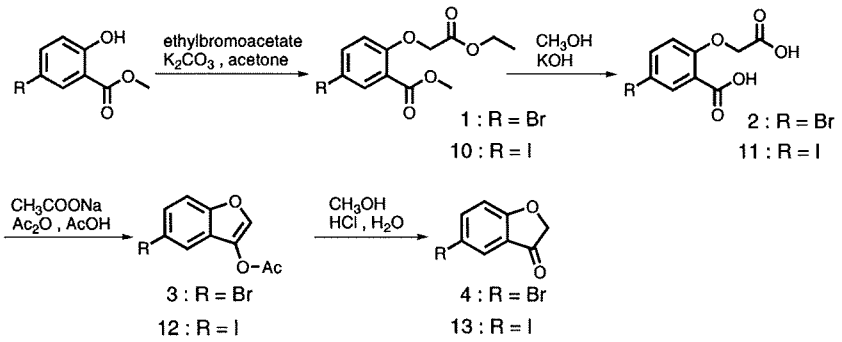

Scheme 2

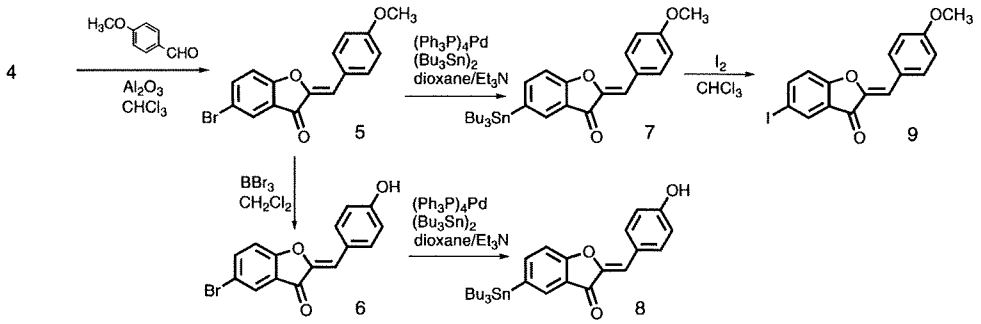

Scheme 3

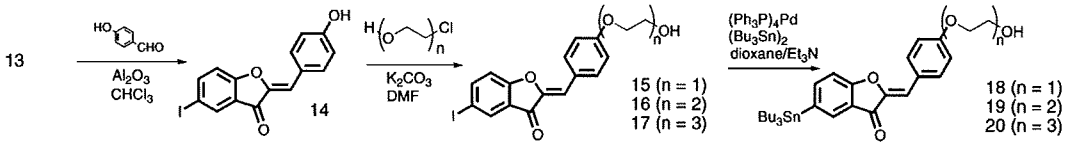

the aurone backbone was achieved by an Aldol reaction of benzofuranones with benzaldehydes using Al_2O_3 (*23*). In this process, benzofuranones were reacted with methoxy benzaldehyde or hydroxy benzaldehyde in the presence of Al_2O_3 in chloroform at room temperature to form compounds **5** and **14** in yields of 85.7% and 87.0%, respectively. Compound **5** was converted to **6** by demethylation with BBr_3 in CH_2Cl_2 (5.2% yields). Direct alkylation of **14** with ethylene chlorohydrin, ethylene glycol mono-2-chloroethyl ether, or 2-[2-(2-chloroethoxy)ethoxy]ethanol with potassium carbonate in DMF resulted in **15**, **16**, and **17**, respectively. The tributyltin derivatives (**7**, **8**, **18**, **19**, and **20**) were prepared from the corresponding compounds (**5**, **6**, **15**, **16**, and **17**) using a halogen to tributyltin exchange reaction catalyzed by Pd(0) for yields of 15.3%, 12.0%, 25.0%, 31.4%, and 30.3%, respectively. The tributyltin derivatives were used as the starting materials for radioiodination in the preparation of [^{125}I]**9**, [^{125}I]**14**, [^{125}I]**15**, [^{125}I]**16**, and [^{125}I]**17**. Novel radioiodinated aurones were achieved by an iododestannylation reaction using hydrogen peroxide as the oxidant, which produced the desired radioiodinated ligands (Scheme 4). It was anticipated that the no-carrier-added preparation would result in a final product bearing a theoretical specific activity similar to that of ^{125}I (2200 Ci/mmol). The radiochemical identities of the radioiodinated ligands were verified by coinjection with nonradioactive compounds by their HPLC profiles (Supporting Information). Five radioiodinated products were obtained in 25−57% radiochemical yields with radiochemical purities of >95% after purification by HPLC.

Binding Experiments Using Aβ Aggregates in Vitro. Our initial screening of the affinity of aurone derivatives (**9**, **14**, **15**, **16**, and **17**) was carried out with Aβ(1−42) aggregates, using

Scheme 4

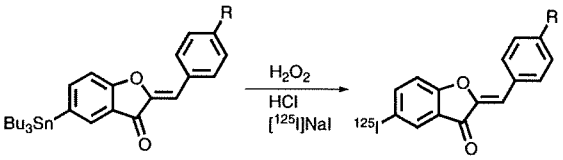

7
8
18
19
20

[^{125}I]9 (R = OCH_3)
[^{125}I]14 (R = OH)
[^{125}I]15 (R = OCH_2CH_2OH)
[^{125}I]16 (R = $(OCH_2CH_2)_2OH$)
[^{125}I]17 (R = $(OCH_2CH_2)_3OH$)

[^{125}I]AAU as the competing radioligand (Table 1). The K_i values estimated for **9**, **14**, **15**, **16**, and **17** were 2.9, 1.3, 1.1, 3.4, and 2.6 nM, respectively. These values suggested that the new series of aurone derivatives had binding affinity for Aβ(1−42) aggregates despite their substituted groups. The binding affinity is in the same range as that of aurone derivatives possessing a nucleophilic group (NH_2, NHMe, NMe_2), reported previously

Table 1. Inhibition Constants (K_i) of Newly Synthesized Aurone Derivatives for the Binding of Ligands to Aβ (1−42) Aggregates

compound	K_i (nM)[a]
9	2.89 ± 0.42
14	1.28 ± 0.29
15	1.05 ± 0.06
16	3.36 ± 0.29
17	2.56 ± 0.31

[a] Data are the mean ± SEM for two independent measurements done in triplicate.

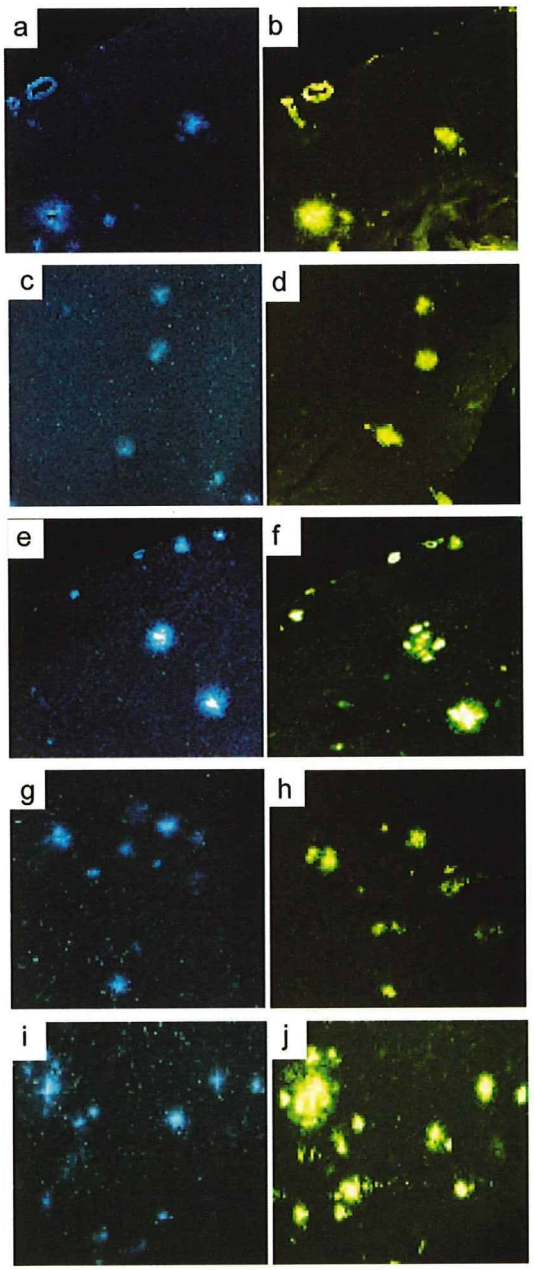

Figure 2. Neuropathological staining of **9**, **14**, **15**, **16**, and **17** (a, c, e, g, and i) in 10 μm sections from a mouse model of AD. Labeled plaques were confirmed by staining of the adjacent sections with thioflavin S (b, d, f, h, and j).

(*19*). These results clearly indicated that there exists considerable tolerance for structural modifications of aurone derivatives. The binding affinity of aurone derivatives is very close to that of known β-amyloid-imaging agents such as SB-13 (K_i = 1.2 nM) (*24*), PIB (K_i = 2.8 nM) (*25*), and IMPY (K_i = 1.4 nM) (*24*), indicating that they have strong enough affinity to test clinically.

Neuropathological Staining of Mouse Brain Sections. To confirm the affinity of aurone derivatives for β-amyloid plaques in the mouse brain, neuropathological fluorescent staining with **9**, **14**, **15**, **16**, and **17** was carried out using double transgenic Alzheimer's mouse brain sections (Figure 2). Many amyloid plaques were clearly stained with the derivatives, as reflected by the high binding affinity for Aβ aggregates in in vitro competition assays. The labeling pattern was consistent with that observed with thioflavin S. These results suggest that novel aurone derivatives show affinity for β-amyloid plaques in the mouse brain in addition to having binding affinity for synthetic Aβ42 aggregates.

Table 2. Biodistribution of Radioactivity after Injection of Aurone Derivatives in Normal Mice[a]

	time after injection (min)			
tissue	2	10	30	60
		[^{125}I]**9**		
blood	3.16 (0.82)	1.51 (0.23)	0.95 (0.19)	0.70 (0.60)
liver	6.87 (2.18)	5.16 (0.73)	2.76 (0.40)	1.86 (0.83)
kidney	7.26 (2.18)	7.00 (1.49)	4.93 (1.52)	2.43 (1.17)
intestine	1.59 (0.51)	4.70 (1.46)	11.67 (3.56)	9.02 (3.14)
spleen	1.45 (0.56)	0.74 (0.10)	0.48 (0.10)	0.43 (0.14)
pancreas	2.83 (0.75)	0.77 (0.17)	0.62 (0.75)	0.16 (0.05)
heart	3.84 (1.04)	1.06 (0.10)	0.37 (0.09)	0.25 (0.12)
stomach[b]	0.39 (0.20)	0.89 (0.48)	0.42 (0.13)	0.82 (0.46)
brain	1.69 (0.43)	0.54 (0.12)	0.11 (0.05)	0.03 (0.02)
		[^{125}I]**14**		
blood	3.14 (0.39)	2.77 (0.28)	1.75 (0.38)	0.87 (0.28)
liver	6.05 (1.49)	6.63 (1.08)	4.23 (0.63)	4.45 (3.14)
kidney	11.08 (2.96)	11.22 (2.26)	5.82 (1.11)	2.43 (1.04)
intestine	2.11 (0.75)	6.12 (0.83)	12.67 (2.13)	14.87 (5.42)
spleen	2.18 (0.48)	1.36 (0.83)	0.69 (0.14)	0.42 (0.02)
pancreas	5.28 (0.99)	2.65 (0.64)	0.92 (0.19)	0.36 (0.09)
heart	6.23 (0.63)	2.57 (0.41)	0.98 (0.14)	0.42 (0.14)
stomach[b]	0.93 (0.28)	1.46 (0.23)	1.22 (0.72)	1.89 (1.01)
brain	3.07 (0.39)	1.48 (0.19)	0.37 (0.07)	0.14 (0.12)
		[^{125}I]**15**		
blood	4.97 (0.96)	3.88 (1.09)	2.38 (0.85)	1.24 (0.35)
liver	13.4 (3.20)	13.3 (2.59)	7.60 (1.95)	5.27 (0.64)
kidney	11.3 (1.23)	10.8 (2.58)	6.09 (2.43)	2.50 (1.30)
intestine	2.78 (0.42)	7.83 (2.22)	17.82 (3.58)	20.93 (4.46)
spleen	2.72 (0.28)	1.02 (0.22)	0.50 (0.13)	0.21 (0.09)
pancreas	6.38 (0.63)	1.61 (0.61)	0.59 (0.21)	0.29(0.15)
heart	6.30 (0.65)	2.30 (0.46)	0.83 (0.15)	0.72 (0.58)
stomach[b]	1.88 (0.41)	3.23 (2.58)	5.15 (4.43)	1.45 (0.78)
brain	4.51 (0.25)	1.48 (0.28)	0.24 (0.03)	0.09 (0.04)
		[^{125}I]**16**		
blood	3.61 (0.74)	5.18 (2.54)	1.11 (0.73)	0.68 (0.45)
liver	12.5 (3.21)	11.6 (1.75)	9.31 (2.66)	7.12 (4.05)
kidney	12.0 (0.99)	10.3 (1.17)	5.75 (1.53)	2.55 (1.12)
intestine	2.35 (1.33)	8.18 (2.32)	19.7 (7.86)	26.38 (5.95)
spleen	2.26 (0.53)	1.56 (0.45)	0.78 (0.26)	0.45 (0.21)
pancreas	5.67(2.72)	2.24 (0.68)	1.40 (0.44)	0.39 (0.29)
heart	6.04 (0.38)	2.77 (0.94)	1.21 (0.66)	0.66 (0.57)
stomach[b]	1.71 (0.38)	5.65 (6.63)	5.00 (2.83)	6.58 (4.59)
brain	3.69 (0.22)	1.53 (0.31)	0.38 (0.05)	0.16 (0.03)
		[^{125}I]**17**		
blood	2.98 (0.64)	4.62 (2.17)	0.83 (0.64)	0.51 (0.31)
liver	12.95 (3.43)	11.20 (1.51)	8.34 (1.98)	7.70 (3.93)
kidney	11.58 (1.13)	9.66 (2.28)	5.84 (1.79)	2.41 (1.22)
intestine	2.52 (0.39)	7.50 (4.85)	17.95 (7.53)	22.64 (5.89)
spleen	2.26 (0.65)	1.40 (0.23)	0.84 (0.23)	0.56 (0.24)
pancreas	5.51 (0.59)	1.84 (0.44)	0.87 (0.37)	0.79 (0.70)
heart	5.67 (1.02)	2.24 (0.56)	1.40 (0.49)	0.39 (0.68)
stomach[b]	3.29 (1.47)	4.73 (5.14)	7.45 (4.62)	7.61 (5.20)
brain	2.81 (0.19)	2.32 (0.21)	0.18 (0.06)	0.08 (0.04)

[a] Expressed as % injected dose per gram. Each value represents the mean (SD) for 4−5 animals. [b] Expressed as % injected dose per organ.

Biodistribution Experiments. To evaluate brain uptake of the aurone derivatives, biodistribution experiments were performed in normal mice with five radioiodinated aurones ([^{125}I]**9**, [^{125}I]**14**, [^{125}I]**15**, [^{125}I]**16**, and [^{125}I]**17**) (Table 2). Radioactivity after injection of the aurone derivatives penetrated the blood−brain barrier showing excellent uptake ranging from 1.7% to 4.5% ID/g brain at 2 min postinjection, a level sufficient for imaging β-amyloid plaques in the brain. In addition, it displayed good clearance from the normal brain with 0.1−0.4% ID/g at 30 min postinjection. Since normal mice were used for the biodistribution experiments, no Aβ plaques were expected in the young mice; therefore, the washout of probes from the brain should be rapid to obtain a higher signal-to-noise ratio earlier in the AD brain. One way to select a ligand with

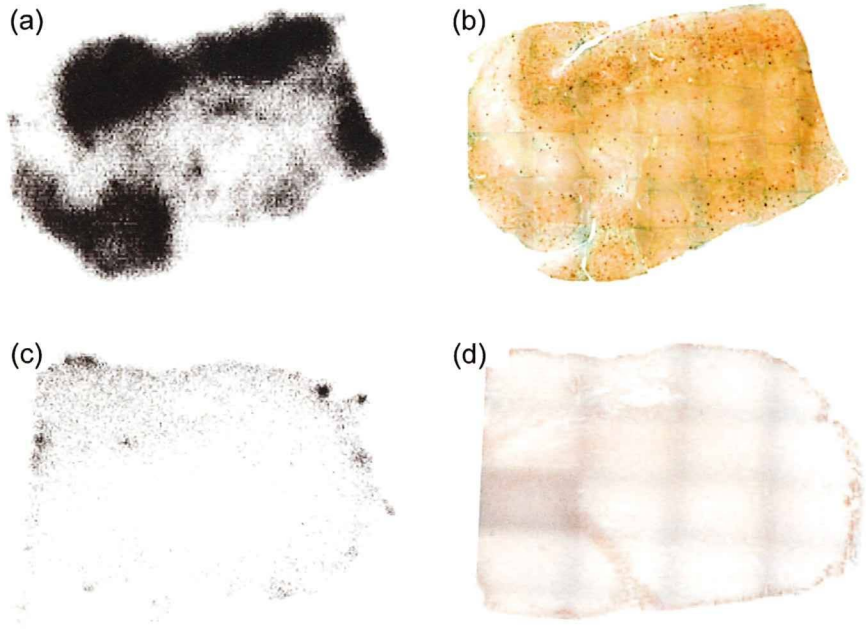

Figure 3. In vitro ARG of [^{125}I]**15** reveals a distinct labeling of amyloid plaques in AD brain sections (a). Under similar conditions, there is very little labeling of [^{125}I]**15** in control brain section (c). The presence and localization of plaques in the sections were confirmed with immunohistochemical staining using a monoclonal Aβ antibody (b, d).

appropriate in vivo kinetics is to use $brain_{2min}/brain_{30min}$ as an index to compare the washout rate. The five radioiodinated aurone derivatives [^{125}I]**9**, [^{125}I]**14**, [^{125}I]**15**, [^{125}I]**16**, and [^{125}I]**17** showed $brain_{2min}/brain_{30min}$ ratios of 15.4, 8.3, 18.8, 9.7, and 15.6, respectively. [^{125}I]**15** had the best washout index. Previously reported radioiodinated aurones showed high uptake (1.9−4.6% ID/g at 2 min postinjection) and good clearance from the brain (0.3−0.5% ID/g at 30 min postinjection) (*19*). However, the $brain_{2min}/brain_{30min}$ ratios of these compounds were 7.3−9.9, lower than that of [^{125}I]**15**, indicating that [^{125}I]**15** could clear more rapidly from the normal mouse brain than aurones with amino groups. It has been reported that [^{123}I]IMPY entered the brain rapidly (2.88% ID at 2 min postinjection) and was cleared from normal brain (0.26% ID at 30 min postinjection), indicating the $brain_{2min}/brain_{30min}$ ratio to be 11.1 (*16*). The aurone derivatives reported in this study appear superior to IMPY in pharmacokinetics, in addition to showing similar binding affinities sufficient for the imaging of β-amyloid plaques in vivo. The pharmacokinetics demonstrated by [^{125}I]**15** is critical to the detection of β-amyloid plaques in the AD brain.

In Vitro Autoradiography. Next, [^{125}I]**15** was investigated for its binding affinity for β-amyloid plaques by in vitro autoradiography in human AD brain sections as shown in Figure 3. Autoradiographic images of [^{125}I]**15** showed high levels of radioactivity in the brain sections (Figure 3a). Furthermore, we confirmed that the hot spots of [^{125}I]**15** corresponded with those of in vitro immunohistochemical staining in the same brain sections (Figure 3b). In contrast, normal human brain displayed no remarkable accumulation of [^{125}I]**15** (Figure 3c), correlating well with the absence of β-amyloid plaques (Figure 3d). These results demonstrate the feasibility of using [^{125}I]**15** as a probe for detecting β-amyloid plaques in the brains of AD patients with SPECT.

CONCLUSION

In conclusion, we successfully designed and synthesized a new series of aurone derivatives as amyloid-imaging agents with high affinity for Aβ(1−42) aggregates in vitro. The derivatives clearly stained amyloid plaques in an animal model of AD, reflecting strong binding to Aβ aggregates in vitro. In biodistribution experiments using normal mice, they displayed good penetration of and fast washout from the brain, especially [^{125}I]**15**. A specific plaque-labeling signal was clearly depicted by [^{125}I]**15** in postmortem AD brain sections. Taken together, the present results suggest [^{125}I]**15** to be a potentially useful probe for the SPECT-based imaging of β-amyloid plaques.

ACKNOWLEDGMENT

This work was supported in part by the Industrial Technology Research Grant Program in 2005 from the New Energy and Industrial Technology Development Organization (NEDO) of Japan and the Program for Promotion of Fundamental Studies in Health Sciences of the National Institute of Biomedical Innovation (NIBIO).

Supporting Information Available: HPLC data of compounds **9**, **14**, **15**, **16**, and **17**. This material is available free of charge via the Internet at http://pubs.acs.org.

LITERATURE CITED

(1) Klunk, W. E. (1998) Biological markers of Alzheimer's disease. *Neurobiol. Aging 19*, 145–7.
(2) Selkoe, D. J. (2001) Alzheimer's disease: genes, proteins, and therapy. *Physiol. Rev. 81*, 741–66.
(3) Selkoe, D. J. (2000) Imaging Alzheimer's amyloid. *Nat. Biotechnol. 18*, 823–4.
(4) Mathis, C. A., Wang, Y., and Klunk, W. E. (2004) Imaging β-amyloid plaques and neurofibrillary tangles in the aging human brain. *Curr. Pharm. Des. 10*, 1469–92.
(5) Nordberg, A. (2004) PET imaging of amyloid in Alzheimer's disease. *Lancet Neurol. 3*, 519–27.
(6) Mathis, C. A., Wang, Y., Holt, D. P., Huang, G. F., Debnath, M. L., and Klunk, W. E. (2003) Synthesis and evaluation of ^{11}C-labeled 6-substituted 2-arylbenzothiazoles as amyloid imaging agents. *J. Med. Chem. 46*, 2740–54.
(7) Klunk, W. E., Engler, H., Nordberg, A., Wang, Y., Blomqvist, G., Holt, D. P., Bergstrom, M., Savitcheva, I., Huang, G. F., Estrada, S., Ausen, B., Debnath, M. L., Barletta, J., Price, J. C., Sandell, J., Lopresti, B. J., Wall, A., Koivisto, P., Antoni, G., Mathis, C. A., and Langstrom, B. (2004) Imaging brain amyloid

in Alzheimer's disease with Pittsburgh compound-B. *Ann. Neurol. 55*, 306–19.

(8) Ono, M., Wilson, A., Nobrega, J., Westaway, D., Verhoeff, P., Zhuang, Z. P., Kung, M. P., and Kung, H. F. (2003) ^{11}C-labeled stilbene derivatives as Aβ-aggregate-specific PET imaging agents for Alzheimer's disease. *Nucl. Med. Biol. 30*, 565–71.

(9) Verhoeff, N. P., Wilson, A. A., Takeshita, S., Trop, L., Hussey, D., Singh, K., Kung, H. F., Kung, M. P., and Houle, S. (2004) In-vivo imaging of Alzheimer disease β-amyloid with [^{11}C]SB-13 PET. *Am. J. Geriatr. Psychiatry 12*, 584–95.

(10) Rowe, C. C., Ackerman, U., Browne, W., Mulligan, R., Pike, K. L., O'Keefe, G., Tochon-Danguy, H., Chan, G., Berlangieri, S. U., Jones, G., Dickinson-Rowe, K. L., Kung, H. P., Zhang, W., Kung, M. P., Skovronsky, D., Dyrks, T., Holl, G., Krause, S., Friebe, M., Lehman, L., Lindemann, S., Dinkelborg, L. M., Masters, C. L., and Villemagne, V. L. (2008) Imaging of amyloid beta in Alzheimer's disease with ^{18}F-BAY94-9172, a novel PET tracer: proof of mechanism. *Lancet Neurol. 7*, 129–35.

(11) Kudo, Y., Okamura, N., Furumoto, S., Tashiro, M., Furukawa, K., Maruyama, M., Itoh, M., Iwata, R., Yanai, K., and Arai, H. (2007) 2-(2-[2-Dimethylaminothiazol-5-yl]ethenyl)-6-(2-[fluoro]ethoxy)benzoxazole: A novel PET agent for in vivo detection of dense amyloid plaques in Alzheimer's disease patients. *J. Nucl. Med. 48*, 553–561.

(12) Agdeppa, E. D., Kepe, V., Liu, J., Flores-Torres, S., Satyamurthy, N., Petric, A., Cole, G. M., Small, G. W., Huang, S. C., and Barrio, J. R. (2001) Binding characteristics of radiofluorinated 6-dialkylamino-2-naphthylethylidene derivatives as positron emission tomography imaging probes for β-amyloid plaques in Alzheimer's disease. *J. Neurosci. 21*, RC189.

(13) Shoghi-Jadid, K., Small, G. W., Agdeppa, E. D., Kepe, V., Ercoli, L. M., Siddarth, P., Read, S., Satyamurthy, N., Petric, A., Huang, S. C., and Barrio, J. R. (2002) Localization of neurofibrillary tangles and β-amyloid plaques in the brains of living patients with Alzheimer disease. *Am. J. Geriatr. Psychiatry 10*, 24–35.

(14) Small, G. W., Kepe, V., Ercoli, L. M., Siddarth, P., Bookheimer, S. Y., Miller, K. J., Lavretsky, H., Burggren, A. C., Cole, G. M., Vinters, H. V., Thompson, P. M., Huang, S. C., Satyamurthy, N., Phelps, M. E., and Barrio, J. R. (2006) PET of brain amyloid and tau in mild cognitive impairment. *N. Engl. J. Med. 355*, 2652–63.

(15) Kung, M. P., Hou, C., Zhuang, Z. P., Zhang, B., Skovronsky, D., Trojanowski, J. Q., Lee, V. M., and Kung, H. F. (2002) IMPY: an improved thioflavin-T derivative for in vivo labeling of beta-amyloid plaques. *Brain Res. 956*, 202–10.

(16) Zhuang, Z. P., Kung, M. P., Wilson, A., Lee, C. W., Plossl, K., Hou, C., Holtzman, D. M., and Kung, H. F. (2003) Structure-activity relationship of imidazo[1,2-a]pyridines as ligands for detecting β-amyloid plaques in the brain. *J. Med. Chem. 46*, 237–43.

(17) Newberg, A. B., Wintering, N. A., Plossl, K., Hochold, J., Stabin, M. G., Watson, M., Skovronsky, D., Clark, C. M., Kung, M. P., and Kung, H. F. (2006) Safety, biodistribution, and dosimetry of ^{123}I-IMPY: a novel amyloid plaque-imaging agent for the diagnosis of Alzheimer's disease. *J. Nucl. Med. 47*, 748–54.

(18) Newberg, A. B., Wintering, N. A., Clark, C. M., Plossl, K., Skovronsky, D., Seibyl, J. P., Kung, M. P., and Kung, H. F. (2006) Use of ^{123}I IMPY SPECT to differentiate Alzheimer's disease from controls. *J. Nucl. Med. 47*, 78P.

(19) Ono, M., Maya, Y., Haratake, M., Ito, K., Mori, H., and Nakayama, M. (2007) Aurones serve as probes of β-amyloid plaques in Alzheimer's disease. *Biochem. Biophys. Res. Commun. 361*, 116–21.

(20) Roberts, M., Bentley, M., and Harris, J. (2002) Chemistry for peptide and protein PEGylation. *Adv. Drug Delivery Rev. 54*, 459–76.

(21) Harris, J., and Chess, R. (2003) Effect of pegylation on pharmaceuticals. *Nat. Rev. Drug Discovery 2*, 214–21.

(22) Cheng, Y., and Prusoff, W. (1973) Relationship between the inhibition constant (K1) and the concentration of inhibitor which causes 50% inhibition (I50) of an enzymatic reaction. *Biochem. Pharmacol.* 3099–3108.

(23) Bryant, W., and Huhn, G. (1995) A practical preparation of 7-methoxy-3(2H)-benzofuranone. *Synth. Commun. 25*, 915–20.

(24) Kung, M. P., Hou, C., Zhuang, Z. P., Skovronsky, D., and Kung, H. F. (2004) Binding of two potential imaging agents targeting amyloid plaques in postmortem brain tissues of patients with Alzheimer's disease. *Brain Res. 1025*, 98–105.

(25) Zhang, W., Oya, S., Kung, M. P., Hou, C., Maier, D. L., and Kung, H. F. (2005) F-18 stilbenes as PET imaging agents for detecting β-amyloid plaques in the brain. *J. Med. Chem. 48*, 5980–8.

BC8003292

Bioorganic & Medicinal Chemistry 17 (2009) 2069–2076

Contents lists available at ScienceDirect

Bioorganic & Medicinal Chemistry

journal homepage: www.elsevier.com/locate/bmc

^{18}F-labeled flavones for in vivo imaging of β-amyloid plaques in Alzheimer's brains

Masahiro Ono [a,b,*], Rumi Watanabe [a], Hidekazu Kawashima [c], Tomoki Kawai [b], Hiroyuki Watanabe [a], Mamoru Haratake [a], Hideo Saji [b], Morio Nakayama [a,*]

[a] Graduate School of Biomedical Sciences, Nagasaki University, 1-14 Bunkyo-machi, Nagasaki 852-8521, Japan
[b] Graduate School of Pharmaceutical Sciences, Kyoto University, 46-29 Yoshida Shimoadachi-cho, Sakyo-ku, Kyoto 606-8501, Japan
[c] Graduate School of Medicine, Kyoto University, Shogoin Kawahara-cho, Sakyo-ku, Kyoto 606-8507, Japan

ARTICLE INFO

Article history:
Received 10 December 2008
Revised 6 January 2009
Accepted 7 January 2009
Available online 20 January 2009

Keywords:
Alzheimer's disease
β-Amyloid plaque
PET
Flavone

ABSTRACT

In vivo imaging of β-amyloid (Aβ) aggregates in the brain may lead to early detection of Alzheimer's disease (AD) and monitoring of the progression and effectiveness of treatment. The purpose of this study was to develop novel ^{18}F-labeled amyloid-imaging probes based on flavones as a core structure. Fluoropegylated (FPEG) flavone derivatives were designed and synthesized. The affinity of the derivatives for Aβ aggregates varied from 5 to 321 nM. In brain sections of AD model mice, FPEG flavones with the dimethylamino group intensely stained β-amyloid plaques. In biodistrubution experiments using normal mice, they displayed high uptake in the brain ranging from 2.9 to 4.2%ID/g at 2 min postinjection. The radioactivity washed out from the brain rapidly (1.3–2.0%ID/g at 30 min), which is highly desirable for β-amyloid imaging agents. FPEG flavones may be potential PET imaging agents for β-amyloid plaques in Alzheimer's brains.

1. Introduction

Alzheimer's disease (AD) is a progressive neurodegenerative disorder characterized by cognitive decline, irreversible memory loss, disorientation, and language impairment. The presence of β-amyloid (Aβ) aggregates in the brain is generally accepted as a hallmark of AD.[1,2] Since the only definitive diagnosis of AD is by pathological examination of postmortem staining of affected brain tissues, the development of techniques which enable one to image β-amyloid plaques in vivo has been strongly desired.[3–5]

Recent success in developing radiolabeled agents targeting Aβ aggregates has provided a window of opportunity to improve the diagnosis of AD. Preliminary reports of positron emission tomography (PET) imaging suggested that [^{11}C]4-*N*-methylamino-4′-hydroxystilbene (SB-13),[6,7] [^{11}C] 2-(4′-(methylaminophenyl)-6-hydroxy benzothiazole (PIB),[8,9] and [^{11}C]2-(2-[2-dimethylaminothiazol-5-yl]ethenyl)-6-(2-[fluoro]ethoxy)benzoxazole (BF-227)[10] showed differential uptake and retention in the brain of AD patients as compared to controls. But ^{11}C is a positron-emitting isotope with a short $t_{1/2}$ (20 min), which limits its clinical application. Recent efforts have focused on the development of comparable agents labeled with a longer half-life isotope, ^{18}F ($t_{1/2}$: 110 min). Preliminary studies with [^{18}F]-2-(1-(2-(*N*-(2-fluoroethyl)-*N*-methylamino)-naphthalen-6-yl)ethylidene)malononitrile ([^{18}F]FDDNP)[11,12] showed differential uptake and retention in the brain of AD patients for the first time. More recently, a stilbene derivative, [^{18}F]BAY94-9172, has been shown to be useful for the imaging of β-amyloid plaques in living human brain tissue in clinical trials.[13]

To search for more candidates for ^{18}F-labeled β-amyloid imaging agents for PET, we planned to evaluate a new series of flavone derivatives previously reported as useful for imaging β-amyloid by single photon emission computed tomography (SPECT).[14] The derivatives showed good affinity for Aβ aggregates in vitro in binding experiments using synthetic Aβ aggregates and neuropathological staining of AD brain sections, suggesting these classes of radioiodinated flavones to be potential imaging agents.

Recently, Kung et al. exploited a novel approach by using fluoro-pegylation (FPEG) of the core structure for ^{18}F labeling of derivatives.[15] Since this approach offers a simple and easy way to incorporate ^{18}F into the target without an appreciable increase in lipophilicity, we planned to apply it to the labeling of flavone derivatives. In addition to the structural characteristics of flavone as the pharmacophore, it has been shown that electron-donating groups such as amino, methylamino, dimethylamino, methoxy, or hydroxy groups play a critical role in the binding of Aβ aggregates.[6,8,16,17] With these considerations, we designed 12 fluorinated flavones with a fluorine or FPEGylation at position 4 and an electron-donating group at position 4′ (Fig. 1).

* Corresponding authors. Tel.: +81 75 753 4608; fax: +81 75 753 4568 (M.O.); tel./fax: +81 95 819 2441 (M.N.).
E-mail addresses: ono@pharm.kyoto-u.ac.jp, mono@net.nagasaki-u.ac.jp (M. Ono) morio@nagasaki-u.ac.jp (M. Nakayama).

0968-0896/$ - see front matter © 2009 Elsevier Ltd. All rights reserved.
doi:10.1016/j.bmc.2009.01.025

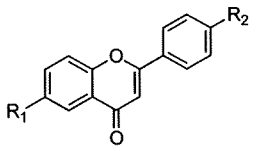

Compound	R_1	R_2
8a	FCH_2CH_2O	$N(CH_3)_2$
8b	$F(CH_2CH_2O)_2$	$N(CH_3)_2$
8c	$F(CH_2CH_2O)_3$	$N(CH_3)_2$
12	FCH_2CH_2O	NH_2
13	FCH_2CH_2O	$NHCH_3$
15b	$F(CH_2CH_2O)_2$	NH_2
15c	$F(CH_2CH_2O)_3$	NH_2
17b	$F(CH_2CH_2O)_2$	$NHCH_3$
17c	$F(CH_2CH_2O)_3$	$NHCH_3$
21	F	NH_2
22	F	$NHCH_3$
23	F	$N(CH_3)_2$

Figure 1. Chemical structure of FPEG-flavone derivatives.

We report here the in vitro and in vivo evaluation of a new series of flavone derivatives as agents for imaging β-amyloid with PET.

2. Experimental

All reagents were commercial products and used without further purification unless otherwise indicated. ^{1}H NMR spectra were obtained on a Varian Gemini 300 spectrometer with TMS as an internal standard. Coupling constants are reported in hertz. Multiplicity is defined by s (singlet), d (doublet), t (triplet), br (broad), and m (multiplet). Mass spectra were obtained on a JEOL IMS-DX instrument.

2.1. Chemistry

2.1.1. 4-Nitrobenzoic acid 2-acetyl-4-methoxyphenyl ester (1)

To a stirring solution of 4-nitrobenzoyl chloride (1.8 g, 10 mmol) in pyridine (20 mL) was added 2-hydroxy-5-methoxyacetophenone (1.6 g, 10 mmol). The reaction mixture was stirred at room temperature for 3 h, and poured into a 1 N aqueous HCl/ice solution with vigorous stirring. The precipitate that formed was filtered and washed with water to yield acetophenone **1** (2.9 g, 90.4% yield). ^{1}H NMR (300 MHz, $CDCl_3$) δ: 2.54 (s, 3H), 3.89 (s, 3H), 7.15–7.16 (m, 2H), 7.38 (d, J = 2.0 Hz, 1H), 8.37 (s, 4H).

2.1.2. 1-(5-Methoxy-2-hydroxyphenyl)-3-(4-nitrophenyl)propane-1,3-dione (2)

A solution of acetophenone **1** (2.9 g, 9.0 mmol) and pyridine (50 mL) was heated to 50 °C, and to it was added pulverized potassium hydroxide (2.5 g, 45.2 mmol). The reaction mixture was stirred for 90 min, and when it had cooled, 30 mL of 10% aqueous acetic acid solution was added. The yellow precipitate that formed was filtered to yield **2** (2.5 g, 88.1% yield). ^{1}H NMR (300 MHz, $CDCl_3$) δ: 3.85 (s, 3H), 6.84 (s, 1H), 6.99 (d, J = 6.9 Hz, 1H), 7.15–7.18 (m, 1H), 7.22 (d, J = 2.2 Hz, 1H), 8.10 (d, J = 6.6 Hz, 2H), 8.35 (d, J = 6.6 Hz, 2H), 11.5 (s, 1H).

2.1.3. 6-Methoxy-4′-nitroflavone (3)

A mixture of the diketone **2** (2.5 g, 8.0 mmol), concentrated sulfuric acid (2 mL), and glacial acetic acid (40 mL) was heated at 100 °C for 2 h and cooled to room temperature. The mixture was poured onto crushed ice, and the resulting precipitate was filtered to yield **3** (1.5 g, 63.5%). ^{1}H NMR (300 MHz, $CDCl_3$) δ: 3.93 (s, 3H), 6.92 (s, 1H), 7.31–7.37 (m, 1H), 7.54–7.61 (m, 2H), 8.11 (d, J = 9.3 Hz, 2H), 8.39 (d, J = 9.3 Hz, 2H).

2.1.4. 6-Methoxy-4′-aminoflavone (4)

A mixture of **3** (3.0 g, 10.2 mmol), $SnCl_2$ (7.6 g, 39.8 mmol), and EtOH (30 mL) was stirred under reflux for 40 min. After the mixture had cooled to room temperature, 1 M NaOH (50 mL) was added until the mixture became alkaline. After extraction with ethyl acetate, the combined organic layers were washed with brine, dried over Na_2SO_4, and filtered. The solvent was removed, and the residue was purified by silica gel chromatography (hexane/ethyl acetate = 1:2) to give 1.3 g of **4** (65.3% yield). ^{1}H NMR (300 MHz, $CDCl_3$) δ: 3.91 (s, 3H), 4.11 (s, broad, 2H), 6.69 (s, 1H), 6.75 (d, J = 6.6 Hz, 2H), 7.24–7.27 (m, 1H), 7.47 (d, J = 6.6 Hz, 1H), 7.59 (d, J = 2.2 Hz, 1H), 7.75 (d, J = 6.6 Hz, 2H).

2.1.5. 6-Methoxy-4′-dimethylaminoflavone (5)

To a mixture of **4** (401 mg, 1.5 mmol) and paraformaldehyde (450 mg, 15 mmol) in AcOH (10 mL) was added $NaCNBH_3$ (471 mg, 7.5 mmol) in one portion at room temperature. The resulting mixture was stirred at room temperature for 1.5 h, and the addition of 1 M NaOH was followed by extraction with CH_3Cl. The organic phase was dried over Na_2SO_4. The solvent was removed, and the residue was purified by silica gel chromatography ($CHCl_3$/MeOH = 20:1) to give 371 mg of **5** (83.7% yield). ^{1}H NMR (300 MHz, $CDCl_3$) δ: 3.07 (s, 6H), 3.91 (s, 3H), 6.70 (s, 1H), 6.75 (d, J = 9.0 Hz, 2H), 7.24–7.26 (m, 1H), 7.47 (d, J = 9.0 Hz, 1H), 7.59 (d, J = 2.2 Hz, 1H), 7.81 (d, J = 9.0 Hz, 2H).

2.1.6. 6-Hydroxy-4′-dimethylaminoflavone (6)

To a solution of **5** (371 mg, 1.5 mmol) in CH_2Cl_2 (10 mL) at 10 °C was added BBr_3 (7.5 mL, 1 M solution in CH_2Cl_2) dropwise in an ice bath. The mixture was allowed to warm to room temperature and was stirred for 12 h. Water was added while the reaction mixture was cooled in an ice bath to keep the reaction temperature at 0 °C. After extraction with CH_2Cl_2, the combined organic phase was dried over Na_2SO_4. The filtrate was concentrated and the residue was purified by silica gel chromatography ($CHCl_3$/MeOH = 20:1) to give 303 mg of **6** (71.8% yield). ^{1}H NMR (300 MHz, $CDCl_3$) δ: 3.05 (s, 6H), 6.74 (d, J = 9.3 Hz, 2H), 7.26 (d, J = 3.0 Hz, 1H), 7.45 (d, J = 9.0 Hz, 1H), 7.58 (d, J = 3.0 Hz, 1H), 7.77 (d, J = 9.0 Hz, 2H).

2.1.7. 6-Hydroxyethoxy-4′-dimethylaminoflavone (7a)

To a solution of **6** (85 mg, 0.30 mmol) and ethylene chlorohydrin (100 μL, 1.50 mmol) in DMSO (3 mL) was added anhydrous K_2CO_3 (41 mg, 0.90 mmol). The reaction mixture was stirred at 120 °C for 48 h, then poured into water. After extraction with chloroform, the organic layers were combined and dried over Na_2SO_4. Evaporation of the solvent afforded a residue, which was purified by silica gel chromatography ($CHCl_3$/MeOH = 33:1) to give 30 mg of **7a** (30.5%). ^{1}H NMR (300 MHz, $CDCl_3$) δ: 3.06 (s, 6H), 3.98–4.05 (m, 2H), 4.17–4.23 (m, 2H), 6.69 (s, 1H), 6.76 (d, J = 9.3 Hz, 2H), 7.28 (d, J = 3.0 Hz, 1H), 7.47 (d, J = 9.0 Hz, 1H), 7.60 (d, J = 3.0 Hz, 1H), 7.80 (d, J = 9.0 Hz, 2H).

2.1.8. 6-(2-(2-Hydroxy-ethoxy)-ethoxy)-4′-dimethylaminoflavone (7b)

To a solution of **6** (82 mg, 0.29 mmol) and ethylene glycol mono-2-chloroethyl ether (37 μL, 0.35 mmol) in DMF (3 mL) was added anhydrous K_2CO_3 (120 mg, 0.87 mmol). The reaction mixture was stirred at 120 °C for 11 h, then poured into water. After extraction with chloroform, the organic layers were combined and dried over Na_2SO_4. Evaporation of the solvent afforded a residue, which was purified by silica gel chromatography (hexane/ethyl acetate = 10:1) to give 107 mg of **7b** (99.3%). ^{1}H NMR (300 MHz, $CDCl_3$) δ: 3.07 (s, 6H), 3.69 (t, J = 5.1 Hz, 2H), 3.79 (s, 2H), 3.91 (t, J = 4.5 Hz, 2H), 4.26 (t, J = 4.5 Hz, 2H), 6.69 (s, 1H), 6.75 (d, J = 9.0 Hz, 2H), 7.27–7.30 (m, 1H), 7.47 (d, J = 9.0 Hz, 1H), 7.64 (d, J = 2.2, 1H), 7.81 (d, J = 9.0 Hz, 2H).

2.1.9. 6-(2-(2-(2-Hydroxy-ethoxy)-ethoxy)ethoxy)-4′-dimethylaminoflavone (7c)

To a solution of **6** (100 mg, 0.36 mmol) and 2-[2-(2-chloroethoxy)ethoxy]ethanol (62 μL, 0.43 mmol) in DMF (3 mL) was added anhydrous K_2CO_3 (148 mg, 1.07 mmol). The reaction mixture was stirred at 120 °C for 17 h, then poured into water. After extraction with chloroform, the organic layers were combined and dried over Na_2SO_4. Evaporation of the solvent afforded a residue, which was purified by preparative TLC ($CHCl_3$/MeOH = 20:1) to give 76 mg of **7c** (51.1%). ^{1}H NMR (300 MHz, $CDCl_3$) δ: 3.07 (s, 6H), 3.62–3.76 (m, 8H), 3.91 (t, J = 4.5 Hz, 2H), 4.26 (t, J = 4.5 Hz, 2H), 6.69 (s, 1H), 6.77 (d, J = 9.3 Hz, 2H), 7.28–7.33 (m, 1H), 7.47 (d, J = 9.0 Hz, 1H), 7.60 (d, J = 2.2, 1H), 7.81 (d, J = 9.0 Hz, 2H).

2.1.10. 6-Fluoroethoxy-4′-dimethylaminoflavone (8a)

To a solution of **7a** (30 mg, 0.09 mmol) in ethylene glycol dimethyl ether (3 mL) was added dimethylamino sulfur trifluoride (DAST) (30 μL, 0.23 mmol) in a dry ice-acetone bath. The reaction mixture was stirred for 6 h at room temperature. The mixture was then poured into a saturated $NaHSO_3$ solution and after extraction with chloroform, the organic phase was separated, dried over Na_2SO_4, and filtered. The residue was purified by silica gel chromatography (hexane/ethyl acetate = 2:1) to give 16 mg of **8a** (53.0%). ^{1}H NMR (300 MHz, $CDCl_3$) δ: 2.93 (s, 6H), 4.26–4.40 (m, 2H), 4.70–4.92 (m, 2H), 6.71 (s, 1H), 6.76 (d, J = 9.0 Hz, 2H), 7.29–7.35 (m, 1H), 7.50 (d, J = 9.0 Hz, 1H), 7.59 (d, J = 3.3 Hz, 1H), 7.82 (d, J = 9.3 Hz, 2H). EI-MS m/z 327 (M^+).

2.1.11. 6-(2-(2-Fluoro-ethoxy)-ethoxy)-4′-dimethylaminoflavone (8b)

To a solution of **7b** (29 mg, 0.08 mmol) in 1,2-dimethoxyethane (DME) (5 mL) was added DAST (21 μL, 0.16 mmol) in a dry ice-acetone bath. The reaction mixture was stirred for 1.5 h at room temperature. The mixture was then poured into a saturated $NaHSO_3$ solution and after extraction with chloroform, after the organic phase was separated, dried over Na_2SO_4, and filtered. The residue was purified by preparative TLC ($CHCl_3$/MeOH = 20:1) to give 15 mg of **8b** (51.5%). ^{1}H NMR (300 MHz, $CDCl_3$) δ: 3.07 (s, 6H), 3.79 (t, J = 4.2 Hz, 1H), 3.89–3.96 (m, 3H), 4.26 (t, J = 4.8 Hz, 2H), 4.54 (t, J = 4.2 Hz), 4.69 (t, J = 4.2 Hz), 6.70 (s, 1H), 6.76 (d, J = 9.0 Hz, 2H), 7.27–7.33 (m, 1H), 7.49 (d, J = 9.3 Hz, 1H), 7.59 (d, J = 3.0, 1H), 7.81 (d, J = 9.0 Hz, 2H). EI-MS m/z 371 (M^+).

2.1.12. 6-(2-(2-(2-Fluoro-ethoxy)-ethoxy)ethoxy)-4′-dimethylaminoflavone (8c)

To a solution of **7c** (141 mg, 0.34 mmol) in DME (5 mL) was added DAST (90 μL, 0.68 mmol) in a dry ice-acetone bath. The reaction mixture was stirred for 1 h at room temperature. The mixture was then poured into saturated $NaHSO_3$ solution and extracted with chloroform. After the organic phase was separated, dried over Na_2SO_4 and filtered, the residue was purified by preparative TLC (hexane/ethyl acetate = 1:5) to give 21 mg of **8c** (14.9%). ^{1}H NMR ($CDCl_3$) δ: 3.08 (s, 6H), 3.69–3.81 (m, 6H), 3.91 (t, J = 4.8 Hz, 2H), 4.24 (t, J = 4.8 Hz, 2H), 4.49 (t, J = 4.5 Hz, 1H), 4.65 (t, J = 4.5 Hz, 1H), 6.69 (s, 1H), 6.76 (d, J = 9.0 Hz, 2H), 7.27–7.33 (m, 1H), 7.48 (d, J = 9.0 Hz, 1H), 7.59 (d, J = 2.2, 1H), 7.81 (d, J = 9.0 Hz, 2H). EI-MS m/z 415 (M^+).

2.1.13. 6-Hydroxy-4′-nitroflavone (9)

The same reaction as described above to prepare **6** was used, and 560 mg of **9** was obtained from **3** and BBr_3. EI-MS m/z 283 (M^+).

2.1.14. 6-(2-Hydroxy-ethoxy)-4′-nitroflavone (10a)

The same reaction as described above to prepare **7a** was used, and 40 mg of **10a** was obtained from **9** in a yield of 9.9%. ^{1}H NMR (300 MHz, $CDCl_3$) δ: 3.88–4.02 (m, 2H), 4.13–4.20 (m, 2H), 6.89 (s, 1H), 7.38–7.41 (m, 1H), 7.59 (d, J = 9.3 Hz, 1H), 7.67 (d, J = 3.3 Hz, 1H), 8.12 (d, J = 9.0 Hz, 2H), 8.46 (d, J = 9.0 Hz, 2H).

2.1.15. 6-(2-(2-Hydroxy-ethoxy)-ethoxy)-4′-nitroflavone (10b)

The same reaction as described above to prepare **7b** was used, and 830 mg of **10b** was obtained from **9**. ^{1}H NMR (300 MHz, $CDCl_3$) δ: 3.70 (t, J = 5.1 Hz, 2H), 3.79 (s, 2H), 3.93 (t, J = 5.0 Hz, 2H), 4.28 (t, J = 4.8 Hz, 2H), 6.90 (s, 1H), 7.37–7.41 (m, 1H), 7.56 (d, J = 9.3 Hz, 1H), 7.66 (d, J = 3.3 Hz, 1H), 8.10 (d, J = 9.0 Hz, 2H), 8.40 (d, J = 9.0 Hz, 2H).

2.1.16. 6-(2-(2-(2-Hydroxy-ethoxy)-ethoxy)ethoxy)-4′-nitroflavone (10c)

The same reaction as described above to prepare **7c** was used, and **10c** was obtained from **9** in a yield of 83.1%. ^{1}H NMR (300 MHz, $CDCl_3$) δ: 3.64 (t, J = 4.5 Hz, 2H), 3.71–3.78 (m, 6H), 3.93 (t, J = 4.8 Hz, 2H), 4.27 (t, J = 4.5 Hz, 2H), 6.90 (s, 1H), 7.38–7.42 (m, 1H), 7.55 (d, J = 9.0 Hz, 1H), 7.61 (d, J = 3.1 Hz, 1H), 8.10 (d, J = 8.7 Hz, 2H), 8.39 (d, J = 8.7 Hz, 2H). EI-MS m/z 415 (M^+).

2.1.17. 6-(2-Fluoro-ethoxy)-4′-nitroflavone (11)

The same reaction as described above to prepare **8a** was used, and 24 mg of **11** was obtained from **10a** in a yield of 41.6%. ^{1}H NMR (300 MHz, $CDCl_3$) 4.26–4.41 (m, 2H), 4.71–4.92 (m, 2H), 6.91 (s, 1H), 7.42–7.44 (m, 1H), 7.56–7.61 (m, 2H), 8.11 (d, J = 9.0 Hz, 2H), 8.39 (d, J = 9.3 Hz, 2H).

2.1.18. 6-(2-Fluoro-ethoxy)-4′-aminoflavone (12)

The same reaction as described above to prepare **4** was used, and 22 mg of **12** was obtained from **11** in a yield of 41.6%. ^{1}H NMR (300 MHz, $CDCl_3$) 4.10 (s, 2H), 4.27–4.39 (m, 2H), 4.71–4.88 (m, 2H), 6.70 (s, 1H), 6.76 (d, J = 9.0 Hz, 2H), 7.29–7.35 (m, 1H), 7.49 (d, J = 9.3 Hz, 1H), 7.58 (s, 1H), 7.75 (d, J = 9.0 Hz, 2H). EI-MS m/z 299 (M^+).

2.1.19. 6-(2-Fluoro-ethoxy)-4′-methylaminoflavone (13)

To a solution of **12** (22 mg, 0.07 mmol) in DMSO (2 mL) were added methyl iodide (0.14 mL) and K_2CO_3 (50.8 mg, 0.37 mmol). The reaction mixture was stirred at room temperature for 5 h, and poured into water (30 mL). After extraction with ethyl acetate (2 × 30 mL), the organic layers were combined and dried over Na_2SO_4. Evaporation of the solvent afforded a residue, which was purified by reversed phase HPLC (acetonitrile/H_2O = 3:2) to give 10 mg of **13** (43.4% yield). ^{1}H NMR (300 MHz, $CDCl_3$) 2.93 (s, 3H), 4.22 (s, 1H), 4.26–4.40 (m, 2H), 4.70–4.91 (m, 2H), 6.71 (s, 1H), 6.76 (d, J = 9.0 Hz, 2H), 7.29–7.35 (m, 1H), 7.50 (d, J = 9.3 Hz, 1H), 7.58 (s, 1H), 7.78 (d, J = 8.7 Hz, 2H). EI-MS m/z 313 (M^+).

2.1.20. 6-(2-(2-Hydroxy-ethoxy)-ethoxy)-4′-aminoflavone (14b)

The same reaction as described above to prepare **4** was used, and 251 mg of **14b** was obtained from **10b** in a yield of 37.9%. ^{1}H NMR ($CDCl_3$) δ: 3.69 (t, J = 5.1 Hz, 2H), 3.79 (s, 2H), 3.91 (t, J = 4.5 Hz, 2H), 4.09 (s, 2H), 4.27 (t, J = 4.2 Hz, 2H), 6.69 (s, 1H), 6.76 (d, J = 8.7 Hz, 2H), 7.27–7.32 (m, 1H), 7.48 (d, J = 9.3 Hz, 1H), 7.65 (d, J = 3.0 Hz, 1H), 7.75 (d, J = 8.4 Hz, 2H). EI-MS m/z 387 (M^+).

2.1.21. 6-(2-(2-(2-Hydroxy-ethoxy)-ethoxy)ethoxy)-4′-aminoflavone (14c)

The same reaction as described above to prepare **4** was used, and 553 mg of **14c** was obtained from **10c** in a yield of 58.8%. ^{1}H NMR (300 MHz, $CDCl_3$) δ: 3.62–3.65 (m, 2H), 3.71–3.78 (m, 6H), 3.91 (t, J = 4.8 Hz, 2H), 4.11 (s, 2H), 4.25 (t, J = 4.5 Hz, 2H), 6.68 (s, 1H), 6.75 (d, J = 8.7 Hz, 2H), 7.27–7.32 (m, 1H), 7.50 (d, J = 9.0 Hz, 1H), 7.59 (d, J = 2.2 Hz, 1H), 7.74 (d, J = 8.7 Hz, 2H). EI-MS m/z 387 (M^+).

2.1.22. 6-(2-(2-Fluoro-ethoxy)-ethoxy)-4′-aminoflavone (15b)

The same reaction as described above to prepare **8b** was used, and 10 mg of **15b** was obtained from **14b** in a yield of 9.1%. ^{1}H NMR ($CDCl_3$) δ: 3.79 (t, J = 4.2 Hz, 1H), 3.86–3.95 (m, 3H), 4.11 (s, 2H), 4.25 (t, J = 4.5 Hz, 2H), 4.53 (t, J = 4.2 Hz, 1H), 4.70 (t, J = 4.2 Hz, 1H), 6.68 (s, 1H), 6.75 (d, J = 9.0 Hz, 2H), 7.28–7.33 (m, 1H), 7.47 (d, J = 9.0 Hz, 1H), 7.58 (d, J = 3.0 Hz, 1H), 7.74 (d, J = 8.4 Hz, 2H). EI-MS m/z 343 (M^+).

2.1.23. 6-(2-(2-(2-Fluoro-ethoxy)-ethoxy)ethoxy)-4′-aminoflavone (15c)

The same reaction as described above to prepare **8** was used, and 85 mg of **15c** was obtained from **14** in a yield of 81.3%. ^{1}H NMR ($CDCl_3$) δ: 3.62–3.65 (m, 2H), 3.70–3.78 (m, 7H), 3.82 (t, J = 3.9 Hz, 1H), 3.90 (t, J = 4.5 Hz, 2H), 4.22 (t, J = 4.5 Hz, 2H), 4.49 (t, J = 4.2 Hz, 1H), 4.66 (t, J = 4.2 Hz, 1H), 6.68 (s, 1H), 6.75 (d, J = 8.7 Hz, 2H), 7.27–7.32 (m, 1H), 7.46 (d, J = 9.3 Hz, 1H), 7.57 (d, J = 2.2 Hz, 1H), 7.73 (d, J = 8.7 Hz, 2H).

2.1.24. 6-(2-(2-Hydroxy-ethoxy)-ethoxy)-4′-methylaminoflavone (16b)

The same reaction as described above to prepare **13** was used, and 41 mg of **16b** was obtained from **14b** in a yield of 37.9%. ^{1}H NMR ($CDCl_3$) δ: 3.49 (s, 3H), 3.69 (t, J = 3.6 Hz, 2H), 3.77–3.79 (m, 2H), 3.91 (t, J = 4.8 Hz, 2H), 4.27 (t, J = 4.0 Hz, 2H), 6.65 (s, 1H), 6.68–6.69 (m, 2H), 7.29–7.32 (m, 1H), 7.47 (d, J = 9.0 Hz, 1H), 7.65 (d, J = 3.0 Hz, 1H), 7.78 (d, J = 9.0 Hz, 2H). EI-MS m/z 355 (M^+).

2.1.25. 6-(2-(2-(2-Hydroxy-ethoxy)-ethoxy)ethoxy)-4′-methylaminoflavone (16c)

The same reaction as described above to prepare **13** was used, and 145 mg of **16c** was obtained from **14c** in a yield of 64.8%. ^{1}H NMR ($CDCl_3$) δ: 2.92 (d, J = 3.0 Hz, 3H), 3.63 (t, J = 5.4 Hz, 2H) 3.72–3.76 (m, 6H), 3.91 (t, J = 5.1 Hz, 2H), 4.25 (t, J = 4.8 Hz, 3H), 6.65 (s, 1H), 6.68 (s, 2H), 7.28–7.32 (m, 1H), 7.46 (d, J = 9.3 Hz, 1H), 7.59 (d, J = 2.2 Hz, 1H), 7.77 (d, J = 8.7 Hz, 2H).

2.1.26. 6-(2-(2-Fluoro-ethoxy)-ethoxy)-4′-methylaminoflavone (17b)

The same reaction as described above to prepare **8** was used, and 9 mg of **17b** was obtained from **16b** in a yield of 21.9%. ^{1}H NMR ($CDCl_3$) δ: 2.93 (d, J = 5.1 Hz, 3H), 3.79 (t, J = 4.2 Hz, 1H), 3.85–3.95 (m, 3H), 4.26 (t, J = 4.8 Hz, 3H), 4.53 (t, J = 4.2 Hz, 1H), 4.70 (t, J = 4.5 Hz, 1H), 6.65 (s, 1H), 6.68 (s, 2H), 7.28–7.32 (m, 1H), 7.47 (d, J = 9.0 Hz, 1H), 7.59 (d, J = 3.0 Hz, 1H), 7.78 (d, J = 9.0 Hz, 2H). EI-MS m/z 357 (M^+).

2.1.27. 6-(2-(2-(2-Fluoro-ethoxy)-ethoxy)ethoxy)-4′-methylaminoflavone (17c)

The same reaction as described above to prepare **8** was used, and 20 mg of **17c** was obtained from **16c** in a yield of 13.8%. ^{1}H NMR ($CDCl_3$) δ: 2.92 (d, J = 4.8 Hz, 3H), 3.69–3.76 (m, 5H), 3.82 (t, J = 4.5 Hz, 1H), 3.91 (t, J = 4.8 Hz, 2H), 4.25 (t, J = 4.2 Hz, 3H), 4.50 (t, J = 4.2 Hz, 1H), 4.66 (t, J = 4.5 Hz, 1H), 6.65 (s, 1H), 6.68 (s, 2H), 7.28–7.31 (m, 1H), 7.46 (d, J = 9.3 Hz, 1H), 7.59 (d, J = 3.0 Hz, 1H), 7.77 (d, J = 8.7 Hz, 2H). EI-MS m/z 401 (M^+).

2.1.28. 4-Nitrobenzoic acid 2-acetyl-4-fluorophenyl ester (18)

The same reaction as described above to prepare **1** was used, and 2.5 g of **18** was obtained from 2-hydroxy-5-fluoroacetophenone and 4-nitrobenzoyl chloride in a yield of 85.6%. ^{1}H NMR (300 MHz, $CDCl_3$) δ: 2.56 (s, 3H), 7.23–7.34 (m, 2H), 7.56–7.60 (m, 1H), 8.37 (s, 4H).

2.1.29. 1-(5-Fluoro-2-hydroxyphenyl)-3-(4-nitrophenyl)propane-1,3-dione (19)

The same reaction as described above to prepare **2** was used, and 2.5 g of **19** was obtained from **18** in a yield of 96.3%. ^{1}H NMR (300 MHz, $CDCl_3$) δ: 6.81 (s, 2H), 7.02 (d, J = 9.0 Hz, 1H), 7.45 (d, J = 9.0 Hz, 1H), 7.68 (s, 1H), 8.11 (d, J = 8.7 Hz, 2H), 8.36 (d, J = 8.7 Hz, 2H), 11.7 (s, 1H).

2.1.30. 6-Fluoro-4′-nitroflavone (20)

The same reaction as described above to prepare **3** was used, and 2.0 g of **20** was obtained from **19** in a yield of 85.3%. EI-MS m/z 285 (M^+).

2.1.31. 6-Fluoro-4′-aminoflavone (21)

The same reaction as described above to prepare **4** was used, and 944 mg of **21** was obtained from **20** in a yield of 67.4%. ^{1}H NMR (300 MHz, $CDCl_3$) δ: 4.13 (s, broad, 2H), 6.74 (s, 1H), 6.76 (d, J = 9.0 Hz, 2H), 7.35–7.42 (m, 1H), 7.51–7.56 (m, 1H), 7.75 (d, J = 8.7 Hz, 2H), 7.82–7.85 (m, 1H).

2.1.32. 6-Fluoro-4′-methylaminoflavone (22)

To a mixture of **21** (300 mg, 1.2 mmol) and paraformaldehyde (179 mg, 5.9 mmol) in MeOH (15 mL) was added a solution of NaOMe (0.34 mL, 28 wt % in MeOH) dropwise at 0 °C. The mixture was stirred under reflux for 1 h. After addition of $NaBH_4$ (246 mg, 6.5 mmol), the solution was heated under reflux for 45 min. To the cold mixture, 1 M NaOH was added followed by extraction with $CHCl_3$. The organic phase was dried over Na_2SO_4 and filtered. The solvent was removed, and the residue was purified by silica gel chromatography (hexane/ethyl acetate = 5:3) to give 314 mg of **22** (99.2%). ^{1}H NMR (300 MHz, $CDCl_3$) δ: 2.91 (s, 3H), 4.37 (s, broad, 1H), 6.63 (s, 1H), 6.66 (s, 2H), 7.32–7.39 (m, 1H), 7.49–7.53 (m, 1H), 7.74 (d, J = 8.7 Hz, 2H), 7.82–7.85 (m, 1H).

2.1.33. 6-Fluoro-4′-dimethylaminoflavone (23)

The same reaction as described above to prepare **5** was used, and 203 mg of **23** was obtained from **21** in a yield of 61.0%. ^{1}H NMR (300 MHz, $CDCl_3$) δ: 3.08 (s, 6H), 6.69 (s, 1H), 6.76 (d, J = 9.3 Hz, 2H), 7.35–7.41 (m, 1H), 7.51–7.56 (m, 1H), 7.81 (d, J = 9.0 Hz, 2H), 7.83–7.86 (m, 1H).

2.1.34. 6-(2-Tosyloxyethoxy)-4′-dimethylaminoflavone (24a)

To a solution of **8a** (136 mg, 0.28 mmol) in pyridine (4 mL) was added tosyl chloride (122 mg, 0.65 mmol) in an ice bath. The reaction mixture was stirred for 32 h at room temperature following the reaction in an ice bath for 1 h. The organic phase was dried over Na_2SO_4 and filtered. The solvent was removed, and the residue was purified by silica gel chromatography (chloroform/MeOH = 20:1) to give 50 mg of **24a** (36.8%). ^{1}H NMR (300 MHz, $CDCl_3$) δ: 2.45 (s, 3H), 3.07 (s, 6H), 4.23 (t, 2H, J = 4.5 Hz), 4.41 (t, J = 5.1 Hz, 2H), 6.68 (s, 1H), 6.75 (d, J = 9.0 Hz, 2H), 7.12–7.18 (m, 1H), 7.35 (d, J = 8.1 Hz, 2H), 7.43–7.56 (m, 2H), 7.82 (t, J = 9.0 Hz, 4H). EI-MS: m/z 479 [M^+].

2.1.35. 6-(2-(2-Tosyloxyethoxy)ethoxy)-4′-dimethylaminoflavone (24b)

The same reaction as described above to prepare **24a** was used, and 111 mg of **24b** was obtained from **8b** in a yield of 34.1%. ^{1}H NMR (300 MHz, $CDCl_3$) δ: 2.41 (s, 3H), 3.08 (s, 6H), 3.76–3.85 (m, 4H), 4.12 (t, J = 5.1 Hz, 2H), 4.22 (t, J = 5.1 Hz, 2H), 6.70 (s, 1H), 6.76 (d, J = 9.0 Hz, 2H), 7.25–7.33 (m, 3H), 7.47 (d, J = 9.0 Hz, 1H), 7.55 (d, J = 3.0 Hz, 1H), 7.79–7.83 (m, 4H). EI-MS m/z 523 (M^+).

2.1.36. 6-(2-(2-(2-Tosyloxyethoxy)ethoxy)ethoxy)-4′-dimethylaminoflavone (24c)

The same reaction as described above to prepare **24a** was used, and 35 mg of **24c** was obtained from **8c** in a yield of 39.9%. ^{1}H NMR (300 MHz, $CDCl_3$) δ: 2.43 (s, 3H), 3.08 (s, 6H), 3.62–3.73 (m, 6H), 3.87 (t, J = 4.8 Hz, 2H), 4.16–4.21 (m, 4H), 6.70 (s, 1H), 6.76 (d, J = 9.0 Hz, 2H), 7.28–7.33 (m, 3H), 7.47 (d, J = 9.0 Hz, 1H), 7.60 (d, J = 2.2 Hz, 1H), 7.79–7.83 (m, 4H). EI-MS m/z 567 (M^+).

2.2. Radiolabeling

[^{18}F]Fluoride produced by an ultracompact cyclotron (CYPRIS model 325R; Sumitomo Heavy Industry Ltd) via an $^{18}O(p,n)^{18}F$ reaction was adsorbed to a strong-base anion exchange resin (Bio-Rad), and was eluted with 500 μL of K_2CO_3 solution (33 mM) into 1 mL of acetonitrile containing Kryptofix 222 (K222) (20 mg). The solvent was removed azeotropically with anhydrous acetonitrile at 120 °C under a nitrogen stream. A solution of tosylate precursor **24(a–c)** (0.2 mg) in 400 μL of DMSO was added to the reaction vessel containing [^{18}F]Fluoride. The mixture was heated at 160 °C for 5 min. The reaction mixture was purified by the reversed phase HPLC system (a Shimadzu LC-6A isocratic pump, a Shimadzu SPD-6A UV detector and an Aloka NDW-351D scitillation detector) on a YMC Hydrosphere C18 column (20 × 150 mm) with acetonitrile/water (70:30) at a flow rate of 9.0 mL/min to obtain [^{18}F]**8(a–c)**. The radiochemical purity and specific activity were determined by analytical HPLC on a YMC Pack Pro C18 column (4.6 × 150 mm, acetonitrile/water (60:40), 1.0 mL/min).

2.3. Binding assays using the aggregated Aβ peptide in solution

A solid form of Aβ(1-42) was purchased from Peptide Institute (Osaka, Japan). Aggregation of peptides was carried out by gently dissolving the peptide (0.25 mg/mL) in a buffer solution (pH 7.4) containing 10 mM sodium phosphate and 1 mM EDTA. The solutions were incubated at 37 °C for 42 h with gentle and constant

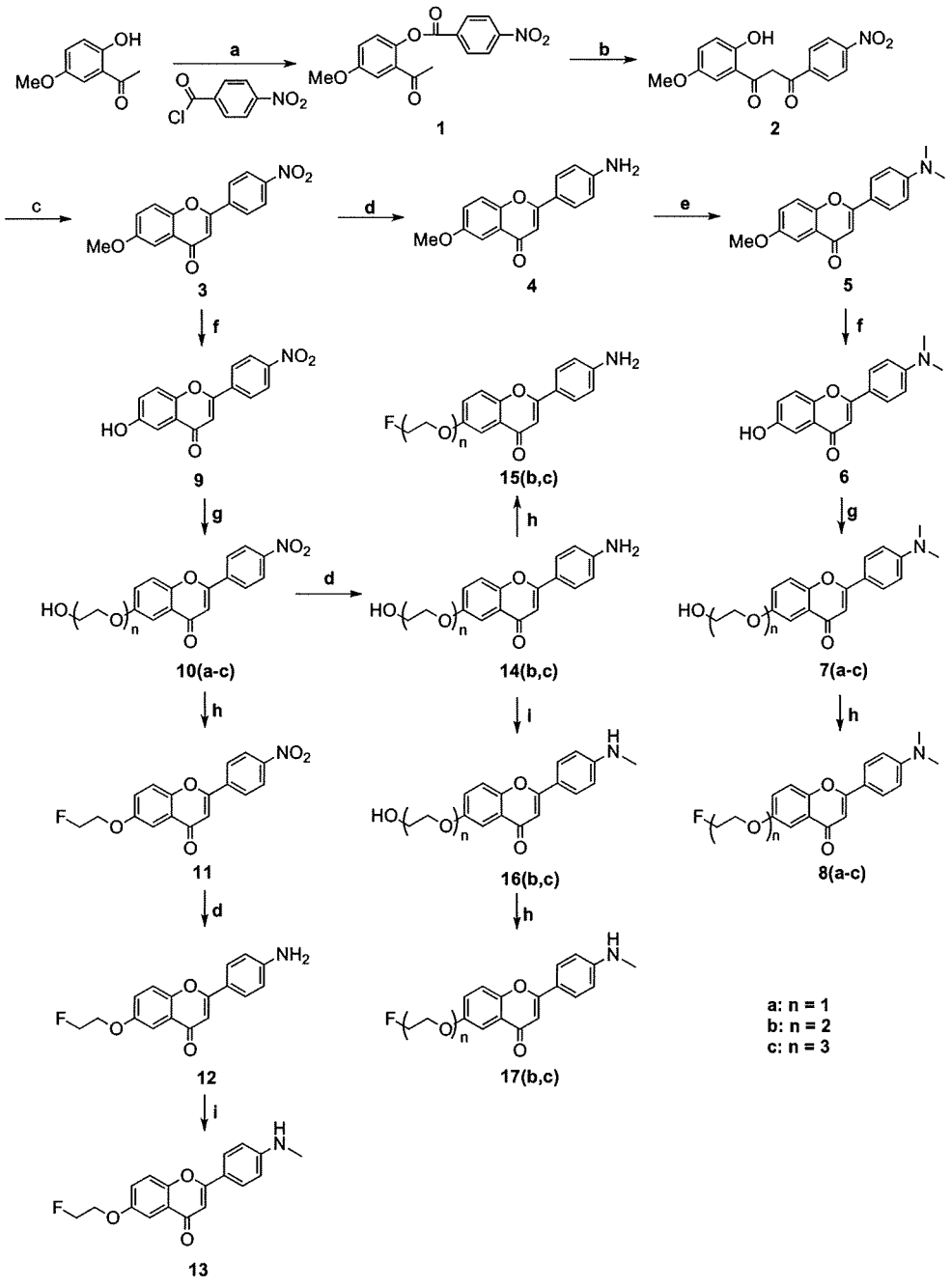

Scheme 1. Reagents: (a) pyridine; (b) KOH, pyridine; (c) H_2SO_4, AcOH; (d) EtOH, $SnCl_2$; (e) $(CH_2O)_n$, $NaCNBH_3$, AcOH; (f) CH_2Cl_2, BBr_3; (g) Cl-(CH2CH2O)n-H (n = 1–3) K_2CO_3, DMF; (h) DAST, DME; (i) DMSO, CH_3I, K_2CO_3.

shaking. Binding experiments were carried out as described previously.[14] [^{125}I]DMFV ([^{125}I]6-iodo-4′-dimethylaminoflavone) with 81.4 TBq/mmol specific activity and greater than 95% radiochemical purity was prepared using the standard iododestannylation reaction.[14] A mixture containing 50 μL of test compounds (0.2 pM-400 μM in 10% EtOH), 50 μL of 0.02 nM [^{125}I]DMFV, 50 μL of Aβ(1-42) aggregates and 850 μL of 10% EtOH was incubated at room temperature for 3 h. The mixture was then filtered through Whatman GF/B filters using a Brandel M-24 cell harvester, and the radioactivity on the filters containing the bound ^{125}I ligand was measured in a gamma counter (Aloka, ARC-380). Values for the half-maximal inhibitory concentration (IC_{50}) were determined from displacement curves of three independent experiments using GraphPad Prism 4.0, and those for the inhibition constant (K_i) were calculated using the Cheng-Prusoff equation:[18] $K_i = IC_{50}/(1 + [L]/K_d)$, where [L] is the concentration of [^{125}I]DMFV used in the assay, and K_d is the dissociation constant of DMFV (12.3 nM).[14]

2.4. Staining of amyloid plaques in transgenic mouse brain sections

Animal studies were conducted in accordance with institutional guidelines and approved by the Kyoto University Animal Care Committee. Tg2576 transgenic mice (female, 20-month-old) were used as an Alzheimer's model. While under isoflurane anesthesia, the mice were sacrificed by decapitation, and the brains were immediately removed and frozen in powdered dry ice. The frozen blocks were sliced into serial sections 10 μm thick using a cryostat (Leica Instruments, CM1900). Each slide was incubated with a 50% ethanol solution (100 μM) of compound **8a**, **8b**, or **8c**, which have the characteristics to emit fluorescence. The sections were washed in 50% ethanol for 3 min two times, and examined using a microscope (Nikon, Eclipse 80i) equipped with a B-2A filter set (excitation, 450–490 nm; dichronic mirror, 505 nm; longpass filter, 520 nm). Thereafter, the serial sections were also immunostained with DAB as a chromogen using monoclonal antibodies against β-amyloid (Amyloid β-Protein Immunohistostain kit, WAKO).

2.5. In vivo biodistribution in normal mice

A saline solution (100 μL) containing ethanol (5 μL) of radiolabeled agents (18.5 kBq) was injected directly into a tail vein of ddY mice (5-week-old, 22–25 g). While under isoflurane anesthesia, the mice were sacrificed at various time points postinjection. The organs of interest were removed and weighed, and radioactivity was measured with an automatic gamma counter (Packard Cobra Auto-Gamma Counter 5003).

3. Results and discussion

The target FPEG flavone derivatives were prepared as shown in Scheme 1. The most common method of synthesizing flavones is known as the Baker-Venkataraman transformation.[19] In this process, a hydroxyacetophenone is first converted into a benzoyl ester **1**, and this species is then treated with a base, forming a 1,3-diketone **2**. Treatment of this diketone with acid leads to generation of the desired flavone **3**. In the route for the synthesis of dimethylamino derivatives, the free amino derivative **4** was readily prepared from **3** by reduction with $SnCl_2$. Compound **5** was converted to **6** by demethylation with BBr_3 in CH_2Cl_2. To prepare compounds with 1-3 ethoxy groups as the PEG linkage, commercially available chlorides were coupled with the OH group of **6** to obtain **7(a–c)**, respectively. The fluorinated flavones, **8(a–c)**, were successfully obtained by reacting **7(a–c)** with DAST in DME or ethylene glycol dimethyl ether. In the route for the synthesis of monomethylated derivatives and the primary amino derivatives, the demethylation of **3** with BBr_3 and the introduction of 1-3 ethoxy groups into **9** gave **10(a–c)**. To prepare

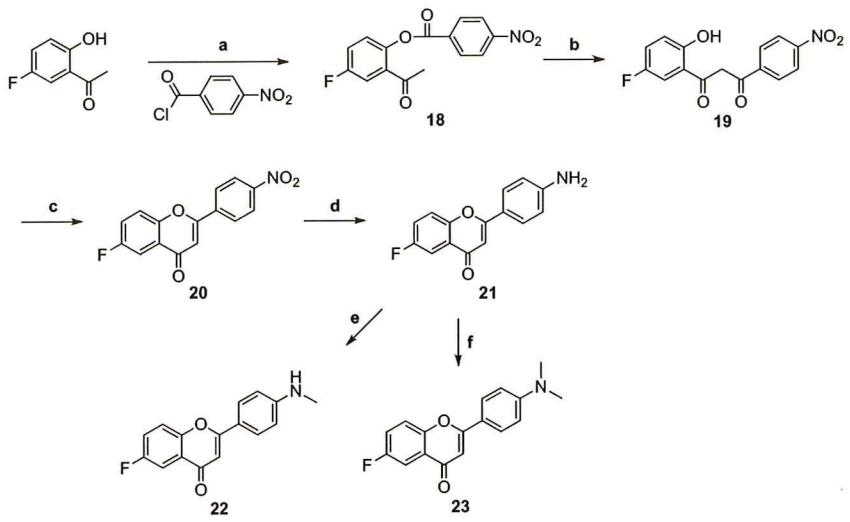

Scheme 2. Reagents: (a) pyridine; (b) KOH, pyridine; (c) H_2SO_4, AcOH; (d) EtOH, $SnCl_2$; (e) $(CH_2O)_n$, NaOMe, $NaBH_4$; (f) $(CH_2O)_n$, $NaCNBH_3$, AcOH.

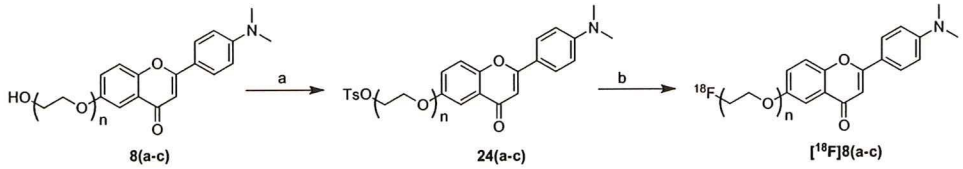

Scheme 3. Reagents: (a) tosyl chloride, pyridine; (b) K_2CO_3, [^{18}F]F^-, kryptofix[222], DMSO/acetonitrile.

the FPEG flavone with one ethoxy group (n = 1) (**12** and **13**), the fluorination of **10a** with DAST, the reduction of **11** with $SnCl_2$ and the methylation of **12** were performed. The primary amino derivatives of FPEG flavones (n = 2 and 3) (**15b** and **15c**) were synthesized by the fluorination of **14b** and **14c** with DAST following the reduction of the nitro group in **10b** and **10c**. The monomethylated FPEG flavones (n = 2 and 3) (**17b** and **17c**) were synthesized by the methylation of **16b** and **16c** following the fluorination of **14b** and **14c** with DAST. We successfully synthesized the flavone derivatives (**21**, **22**, and **23**) with fluorine directly bound to the phenyl group according to a procedure reported previously (Scheme 2). To make the desired ^{18}F-labeled FPEG flavones, [^{18}F]**8(a–c)**, the tosylates **24(a–c)** were employed as the precursors. The free OH groups of **8(a–c)** were converted into tosylates by reacting with TsCl in the presence of pyridine to give **24(a–c)** (Scheme 3). Each of the tosylates, **24(a–c)**, was mixed with [^{18}F]fluoride/potassium carbonate and Kryptofix 222 in DMSO and heated at 160 °C for 5 min. The crude product was purified by HPLC (radiochemical purity >99%, radiochemical yield 5–13%, decay corrected). The total synthesis time was 70 min, and the specific activity was estimated to be 33.3–55.5 GBq/mmol at the end of synthesis.

Table 1
Inhibition constants (K_i, nM) of compounds for the binding of [^{125}I]DMFV to Aβ(1-42) aggregates[a]

Compound	K_i (nM)	Compound	K_i (nM)
8a	5.3 ± 0.8	**15c**	234.0 ± 60.6
8b	14.4 ± 2.5	**17b**	54.5 ± 10.3
8c	19.3 ± 4.0	**17c**	45.1 ± 5.8
12	234.3 ± 63.5	**21**	260.5 ± 43.3
13	99.0 ± 11.8	**22**	110.0 ± 47.4
15b	321.1 ± 74.4	**23**	73.9 ± 5.3

[a] Values are the mean ± standard error of the mean for 4–9 experiments.

Table 2
Biodistribution of ^{18}F-labeled flavones in normal mice[a]

Organ	2 min	10 min	30 min	60 min
*[^{18}F]**8a***				
Blood	2.80 ± 0.41	2.71 ± 0.13	2.53 ± 0.17	3.25 ± 0.31
Brain	4.17 ± 0.77	3.62 ± 0.21	1.89 ± 0.13	2.19 ± 0.18
Bone	2.02 ± 0.53	2.83 ± 0.23	4.51 ± 0.55	6.21 ± 0.84
*[^{18}F]**8b***				
Blood	2.09 ± 0.35	2.30 ± 0.07	2.50 ± 0.21	2.94 ± 0.27
Brain	3.54 ± 0.54	2.75 ± 0.21	2.00 ± 0.20	2.13 ± 0.10
Bone	1.13 ± 0.22	1.65 ± 0.10	2.42 ± 0.38	3.74 ± 0.30
*[^{18}F]**8c***				
Blood	2.35 ± 0.54	1.50 ± 0.26	1.40 ± 0.04	1.88 ± 0.08
Brain	2.89 ± 0.74	2.23 ± 0.36	1.31 ± 0.14	1.37 ± 0.11
Bone	1.53 ± 0.52	2.38 ± 0.39	4.06 ± 0.49	5.21 ± 0.98

[a] Expressed as % of injected dose per gram. Each value represents the mean ± SD for 4–5 mice at each interval.

In vitro binding experiments to evaluate the affinity of the FPEG flavones for Aβ aggregates were carried out in solutions with [^{125}I]DMFV as the ligand. The affinity of flavone derivatives for Aβ aggregates varied from 5 to 321 nM (Table 1). The flavone derivatives had affinity for Aβ(1-42) aggregates in the following order: the dimethyamino derivatives (**8a**, **8b**, **8c**, and **23**) > the monomethylamino derivatives (**13**, **17b**, **17c**, and **22**) > the primary amino derivatives (**12**, **15b**, **15c**, and **21**). The results of the binding experiments are consistent with those of previous reports.[14,20,21] The K_i values indicated that the affinity for Aβ(1-42) aggregates was affected by the substituted group at position 4′ in the flavone structure, not by the length of the PEG introduced into the flavone backbone. We selected the dimethylamino derivatives (**8a**, **8b**, and **8c**), which showed greater binding affinity than the monomethylamino derivatives and the primary amino derivatives, for additional study.

Three ^{18}F FPEG flavones ([^{18}F]**8a**, [^{18}F]**8b**, and [^{18}F]**8c**) were examined for their biodistribution in normal mice (Table 2). All three ligands displayed high uptake from the brain 2.89–4.17%ID/g, at 2 min postinjection, indicating a level sufficient for imaging. In addition, they displayed good clearance from the normal brain with 1.89, 2.00, and 1.31%ID/g at 30 min postinjection for [^{18}F]**8a**, [^{18}F]**8b**, and [^{18}F]**8c**, respectively. These values were equal to 45.3%, 56.5%, and 45.3% of the initial uptake peak for [^{18}F]**8a**, [^{18}F]**8b**, and [^{18}F]**8c**, respectively. A rapid initial uptake in normal brain coupled with a fast washout are highly desirable properties for β-amyloid-imaging probes, as they lead to a high signal to background ratio. [^{18}F]**8(a–c)** showed the bone uptake (3.74–6.21%ID/g) at 60 min postinjection, suggesting there may be in vivo defluorination. However, the free fluorine was not taken up by brain tissue; therefore, the interference from this free fluoride is expected to be relatively low for brain imaging.[22]

To confirm the affinity of FPEG chalcone derivatives for β-amyloid plaques in the brain, neuropathological fluorescent staining

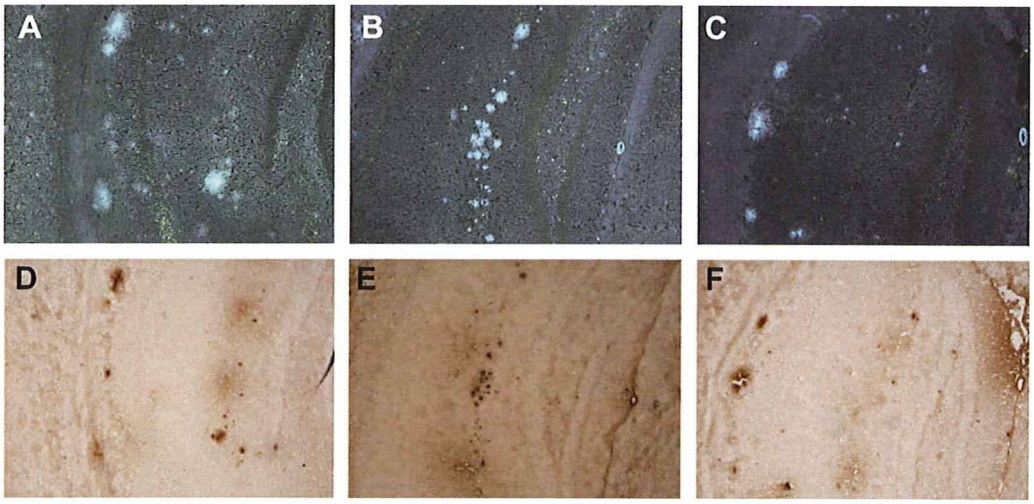

Figure 2. Neuropathological staining of flavone derivatives **8a** (A), **8b** (B), and **8c** (C) in 10-μm brain sections of Tg2576 mice. Immunohistological staining with an antibody against β-amyloid (D, E, and F) in the adjacent sections of A, B, and C, respectively.

with **8a**, **8b**, and **8c** was carried out using the Alzheimer's model (Fig. 2A–C). Many fluorescence spots were observed in the brain sections of Tg2576 transgenic (female, 20-month-old) mice, while no spots were observed in the brain sections of wild-type (female, 22-month-old) mice (data not shown). The fluorescent labeling pattern was consistent with that obtained by immunohistochemical labeling with an antibody specific for Aβ (Fig. 2D–F), indicating that FPEG flavones show specific binding to β-amyloid plaques in the mouse brain.

In conclusion, we successfully designed and synthesized novel ^{18}F labeled flavones with the FPEG strategy for PET imaging of β-amyloid in the brain. The affinity of the derivatives for Aβ aggregates varied from 5 to 321 nM. When in vitro plaque labeling was carried out using sections of brain from Tg2576 mice, FPEG flavones intensely stained β-amyloid plaques. In addition, they displayed good uptake into and a rapid washout from the brain after injection in normal mice. The combination of high binding affinity for β-amyloid plaques, high brain uptake, and good clearance in mice of the FPEG-flavone derivatives may provide a series of promising in vivo amyloid imaging agents for PET.

Acknowledgments

This study was supported by the Industrial Technology Research Grant Program from the New Energy and Industrial Technology Development Organization (NEDO) of Japan, and the Program for Promotion of Fundamental Studies in Health Sciences of the National Institute of Biomedical Innovation (NIBIO).

References and notes

1. Hardy, J. A.; Higgins, G. A. *Science* **1992**, *256*, 184.
2. Selkoe, D. J. *Physiol. Rev.* **2001**, *81*, 741.
3. Selkoe, D. J. *Nat. Biotechnol.* **2000**, *18*, 823.
4. Mathis, C. A.; Wang, Y.; Klunk, W. E. *Curr. Pharm. Des.* **2004**, *10*, 1469.
5. Nordberg, A. *Lancet Neurol.* **2004**, *3*, 519.
6. Ono, M.; Wilson, A.; Nobrega, J.; Westaway, D.; Verhoeff, P.; Zhuang, Z. P.; Kung, M. P.; Kung, H. F. *Nucl. Med. Biol.* **2003**, *30*, 565.
7. Verhoeff, N. P.; Wilson, A. A.; Takeshita, S.; Trop, L.; Hussey, D.; Singh, K.; Kung, H. F.; Kung, M. P.; Houle, S. *Am. J. Geriatr. Psychiat.* **2004**, *12*, 584.
8. Mathis, C. A.; Wang, Y.; Holt, D. P.; Huang, G. F.; Debnath, M. L.; Klunk, W. E. *J. Med. Chem.* **2003**, *46*, 2740.
9. Klunk, W. E.; Engler, H.; Nordberg, A.; Wang, Y.; Blomqvist, G.; Holt, D. P.; Bergstrom, M.; Savitcheva, I.; Huang, G. F.; Estrada, S.; Ausen, B.; Debnath, M. L.; Barletta, J.; Price, J. C.; Sandell, J.; Lopresti, B. J.; Wall, A.; Koivisto, P.; Antoni, G.; Mathis, C. A.; Langstrom, B. *Ann. Neurol.* **2004**, *55*, 306.
10. Kudo, Y.; Okamura, N.; Furumoto, S.; Tashiro, M.; Furukawa, K.; Maruyama, M.; Itoh, M.; Iwata, R.; Yanai, K.; Arai, H. *J. Nucl. Med.* **2007**, *48*, 553.
11. Agdeppa, E. D.; Kepe, V.; Liu, J.; Flores-Torres, S.; Satyamurthy, N.; Petric, A.; Cole, G. M.; Small, G. W.; Huang, S. C.; Barrio, J. R. *J. Neurosci.* **2001**, *21*, RC189.
12. Shoghi-Jadid, K.; Small, G. W.; Agdeppa, E. D.; Kepe, V.; Ercoli, L. M.; Siddarth, P.; Read, S.; Satyamurthy, N.; Petric, A.; Huang, S. C.; Barrio, J. R. *Am. J. Geriatr. Psychiat.* **2002**, *10*, 24.
13. Rowe, C. C.; Ackerman, U.; Browne, W.; Mulligan, R.; Pike, K. L.; O'Keefe, G.; Tochon-Danguy, H.; Chan, G.; Berlangieri, S. U.; Jones, G.; Dickinson-Rowe, K. L.; Kung, H. P.; Zhang, W.; Kung, M. P.; Skovronsky, D.; Dyrks, T.; Holl, G.; Krause, S.; Friebe, M.; Lehman, L.; Lindemann, S.; Dinkelborg, L. M.; Masters, C. L.; Villemagne, V. L. *Lancet Neurol.* **2008**, *7*, 129.
14. Ono, M.; Yoshida, N.; Ishibashi, K.; Haratake, M.; Arano, Y.; Mori, H.; Nakayama, M. *J. Med. Chem.* **2005**, *48*, 7253.
15. Stephenson, K. A.; Chandra, R.; Zhuang, Z. P.; Hou, C.; Oya, S.; Kung, M. P.; Kung, H. F. *Bioconjugate Chem.* **2007**, *18*, 238.
16. Ono, M.; Kung, M. P.; Hou, C.; Kung, H. F. *Nucl. Med. Biol.* **2002**, *29*, 633.
17. Zhuang, Z. P.; Kung, M. P.; Wilson, A.; Lee, C. W.; Plossl, K.; Hou, C.; Holtzman, D. M.; Kung, H. F. *J. Med. Chem.* **2003**, *46*, 237.
18. Cheng, Y.; Prusoff, W. *Biochem. Pharmacol.* **1973**, *1973*, 3099.
19. Ares, J. J.; Outt, P. E.; Randall, J. L.; Murray, P. D.; Weisshaar, P. S.; O'Brien, L. M.; Ems, B. L.; Kakodkar, S. V.; Kelm, G. R.; Kershaw, W. C., et al *J. Med. Chem.* **1995**, *38*, 4937.
20. Ono, M.; Haratake, M.; Mori, H.; Nakayama, M. *Bioorg. Med. Chem.* **2007**, *15*, 6802.
21. Ono, M.; Hori, M.; Haratake, M.; Tomiyama, T.; Mori, H.; Nakayama, M. *Bioorg. Med. Chem.* **2007**, *15*, 6388.
22. Zhang, W.; Oya, S.; Kung, M. P.; Hou, C.; Maier, D. L.; Kung, H. F. *Nucl. Med. Biol.* **2005**, *32*, 799.

Bioorganic & Medicinal Chemistry 17 (2009) 6402–6406

Contents lists available at ScienceDirect

Bioorganic & Medicinal Chemistry

journal homepage: www.elsevier.com/locate/bmc

Synthesis and biological evaluation of radioiodinated 2,5-diphenyl-1,3,4-oxadiazoles for detecting β-amyloid plaques in the brain

Hiroyuki Watanabe [a], Masahiro Ono [a,b,*], Ryoichi Ikeoka [a], Mamoru Haratake [a], Hideo Saji [b], Morio Nakayama [a,*]

[a] Graduate School of Biomedical Sciences, Nagasaki University, 1-14 Bunkyo-machi, Nagasaki 852-8521, Japan
[b] Graduate School of Pharmaceutical Sciences, Kyoto University, 46-29 Yoshida Shimoadachi-cho, Sakyo-ku, Kyoto 606-8501, Japan

ARTICLE INFO

Article history:
Received 2 June 2009
Revised 10 July 2009
Accepted 11 July 2009
Available online 17 July 2009

Keywords:
Alzheimer's disease
β-Amyloid plaques
SPECT imaging

ABSTRACT

This paper describes the synthesis and biological evaluation of a new series of 2,5-diphenyl-1,3,4-oxadiazole (1,3,4-DPOD) derivatives for detecting β-amyloid plaques in Alzheimer's brains. The affinity for β-amyloid plaques was assessed by an in vitro binding assay using pre-formed synthetic Aβ42 aggregates. The new series of 1,3,4-DPOD derivatives showed affinity for Aβ42 aggregates with K_i values ranging from 20 to 349 nM. The 1,3,4-DPOD derivatives clearly stained β-amyloid plaques in an animal model of Alzheimer's disease, reflecting the affinity for Aβ42 aggregates in vitro. Compared to 3,5-diphenyl-1,2,4-oxadiazole (1,2,4-DPOD) derivatives, they displayed good penetration of and fast washout from the brain in biodistribution experiments using normal mice. The novel radioiodinated 1,3,4-DPOD derivatives may be useful probes for detecting β-amyloid plaques in the Alzheimer's brain.

1. Introduction

Alzheimer's disease (AD) is a progressive neurodegenerative disorder pathologically characterized by the deposition of β-amyloid (Aβ) peptides as senile plaques in the brain.[1,2] Since the deposition of Aβ plaques is an early event in the development of AD, a validated biomarker of Aβ deposition in the brain would likely prove useful for identifying and following individuals at risk for AD and assist in the evaluation of new anti-amyloid therapies currently under development. Therefore, the quantitative evaluation of Aβ plaques in the brain with non-invasive techniques such as positron emission tomography (PET) and single photon emission computed tomography (SPECT) could lead to the presymptomatic detection of AD and new anti-amyloid therapies.[3–5]

In the past few years, several groups have reported potential Aβ-imaging probes for the detection of Aβ plaques in vivo. Tracers such as [^{11}C]PIB,[6,7] [^{11}C]SB-13,[8,9] [^{18}F]BAY94-9172,[10] [^{11}C]BF-227,[11] [^{18}F]FDDNP,[12–14] and [^{123}I]IMPY[15–18] have been tested clinically and demonstrated utility. [^{123}I]IMPY is the only tracer for SPECT, the other five tracers are Aβ-imaging probes for PET. Since SPECT is more valuable than PET in terms of routine diagnostic use, the development of more useful Aβ-imaging agents for SPECT has been a critical issue.

Recently, we successfully designed and synthesized a new series of 3,5-diphenyl-1,2,4-oxadiazole (1,2,4-DPOD) derivatives as SPECT probes for the in vivo imaging of Aβ plaques in the brain.[19] The 1,2,4-DPOD derivatives are categorized into Aβ-imaging agents with the three-aromatic-ring linked system.[20–22] The derivatives displayed excellent affinity for Aβ aggregates in in vitro binding experiments. The degree to which the DPOD derivatives penetrated the brain was also very encouraging. However, nonspecific binding in vivo reflected by a slow washout from the normal mouse brain makes them unsuitable for the imaging of Aβ plaques. The less than ideal in vivo biodistribution results in normal mice indicate that there is a critical need to fine-tune the kinetics of brain uptake and washout. Additional structural changes, that is, reducing the lipophilicity, are necessary to improve the in vivo properties of the DPOD derivatives.

In an attempt to further develop novel ligands for the imaging of Aβ plaques in AD, we designed a series of 2,5-diphenyl-1,3,4-oxadiazole (1,3,4-DPOD) derivatives, which are structural isomers of 1,2,4-DPOD and less lipophilic than 1,2,4-DPOD (Fig. 1). To our

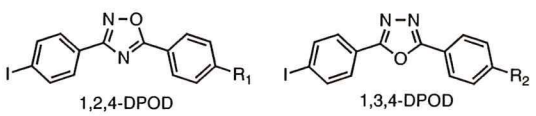

Figure 1. Chemical structure of 1,2,4-DPOD reported previously and 1,3,4-DPOD reported in this paper. R_1 = NH_2, $NHCH_3$, $N(CH_3)_2$, OCH_3, OH; R_2 = $N(CH_3)_2$, OCH_3, OH, OCH_2CH_2OH, $(OCH_2CH_2)_2OH$, $(OCH_2CH_2)_3OH$.

* Corresponding authors. Tel.: +81 75 753 4608; fax: +81 75 753 4568 (M.O.); tel./fax: +81 95 819 2441 (M.N.).
E-mail addresses: ono@pharm.kyoto-u.ac.jp (M. Ono), morio@nagasaki-u.ac.jp (M. Nakayama).

0968-0896/$ - see front matter © 2009 Elsevier Ltd. All rights reserved.
doi:10.1016/j.bmc.2009.07.020

knowledge, this is the first time the use of 1,3,4-DPOD derivatives in vivo as probes to image Aβ plaques in the AD brain has been proposed. Described herein is the synthesis of a novel series of 1,3,4-DPOD derivatives and the characterization as Aβ-imaging probes in comparison with 1,2,4-DPOD derivatives.

2. Results and discussion

The synthesis of 1,3,4-DPOD derivatives is outlined in Schemes 1 and 2. We used the one-pot synthesis method of producing 2,5-diphenyl-1,3,4-oxadiazoles.[23] The 2,5-diphenyl-1,3,4-oxadiazoles (**3** and **4**) were prepared by 4-iodobenzhydrazide with 4-dimethylaminobenzaldehyde and 4-methoxybenzaldehyde in the presence of ceric ammonium nitrate (CAN). Compound **4** was converted to **6** by demethylation with BBr_3 in CH_2Cl_2 (49% yield). Direct alkylation of **6** with ethylene chlorohydrin, ethylene glycol mono-2-chloroethyl ether, or 2-[2-(2-chloroethoxy)ethoxy]ethanol with potassium carbonate in DMF resulted in **7–9**. The tributyltin derivatives (**2** and **5**) were prepared from corresponding compounds (**1** and **4**) using a halogen to tributyltin exchange reaction catalyzed by Pd(0) for yields of 8.2% and 6.5%, respectively. The tributyltin derivatives were used as the starting materials for radioiodination in the preparation of [^{125}I]**3** and [^{125}I]**4**. Novel radioiodinated 1,3,4-DPOD derivatives were obtained by an iododestannylation reaction using hydrogen peroxide as the oxidant which produced the desired radioiodinated ligands (Scheme 3). It was anticipated that the no-carrier-added preparation would result in a final product bearing a theoretical specific activity similar to that of ^{125}I (2200 Ci/mmol). The radiochemical identity of the radioiodinated ligands was verified by co-injection with non-radioiodinated compounds from their HPLC profiles. [^{125}I]**3** and [^{125}I]**4** were each obtained in a radiochemical yield of >45% with a radiochemical purity of >95% after purification by HPLC.

The affinity of 1,3,4-DPOD derivatives (**3**, **4**, **6–9**) was evaluated based on inhibition of the binding of [^{125}I]IMPY to Aβ42 aggregates. As shown in Table 1, all 1,3,4-DPOD derivatives showed inhibitory activity toward Aβ aggregates. The affinity of 1,3,4-DPOD derivatives for Aβ aggregates varied from 20 to 349 nM. Compound **3** with the dimethylamino group and **4** with the methoxy group showed high binding affinity with a K_i of 20 and 46 nM, respectively, while no marked affinity was observed for **6–9**. Compound **3** displayed almost equal affinity for Aβ aggregates as the 1,2,4-DPOD derivative with the dimethylamino group (4-(3-(4-iodophenyl)-1,2,4-oxadiazole-5-yl)-*N*,*N*-dimethylamine; 1,2,4-DPOD-DM, K_i = 15 nM).[19]

To confirm the affinity of 1,3,4-DPOD derivatives for Aβ plaques in the brain, fluorescent staining of sections of mouse brain from an animal model of AD was carried out with compound **3** (Fig. 2). Many fluorescence spots were observed in the brain sections of Tg2576 transgenic mice (female, 28-month-old) (Fig. 2A), while no spots were observed in the brain sections of wild-type mice (female, 28-month-old) (Fig. 2B). The fluorescent labeling pattern was consistent with that observed with thioflavin S (Fig. 2C). These results suggested that **3** shows specific binding to Aβ plaques in the mouse brain. In the fluorescent staining of Tg2576 mouse brain sections, **4** also showed specific binding to Aβ plaques in the brain (data not shown).

Next, [^{125}I]**3** and [^{125}I]**4** were evaluated for their in vivo biodistribution in normal mice. A biodistribution study provides critical information on brain penetration. Generally, a freely diffusible compound with an optimal log *P* value of 2–3 will have an initial brain uptake of 2–3% dose/whole brain at 2 min after iv injection. [^{125}I]**3** and [^{125}I]**4** examined in this study displayed optimal lipophilicity as reflected by log *P* values of 2.43 and 2.58, respectively (Table 2). As expected, these ligands displayed good brain uptake ranging from 3.8% to 5.9% ID/g brain at 2–10 min postinjection, indicating a level sufficient for brain imaging probes (Table 3). In addition, they displayed good clearance from the normal brain with 1.8% and 0.36% ID/g at 60 min postinjection for [^{125}I]**3** and [^{125}I]**4**, respectively. These values were equal to a peak in brain uptake of 30% and 9.6%, respectively. Additionally, all of the other organs or tissues displayed a good initial uptake and a relatively fast washout with time. To directly compare the brain uptake and washout of [^{125}I]1,2,4-DPOD and [^{125}I]1,3,4-DPOD, a combined plot is presented in Figure 3. It is apparent that [^{125}I]1,2,4-DPOD showed a lower initial uptake with a longer retention, while [^{125}I]1,3,4-DPOD displayed a higher initial uptake but with a faster washout from the brain. At 2 or 10 min after iv injection, the uptake of [^{125}I]1,3,4-DPOD reached a maximum after which the activity in the normal brain was washed out. It is important to note that

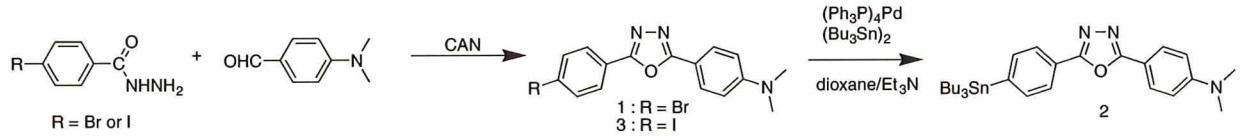

Scheme 1.

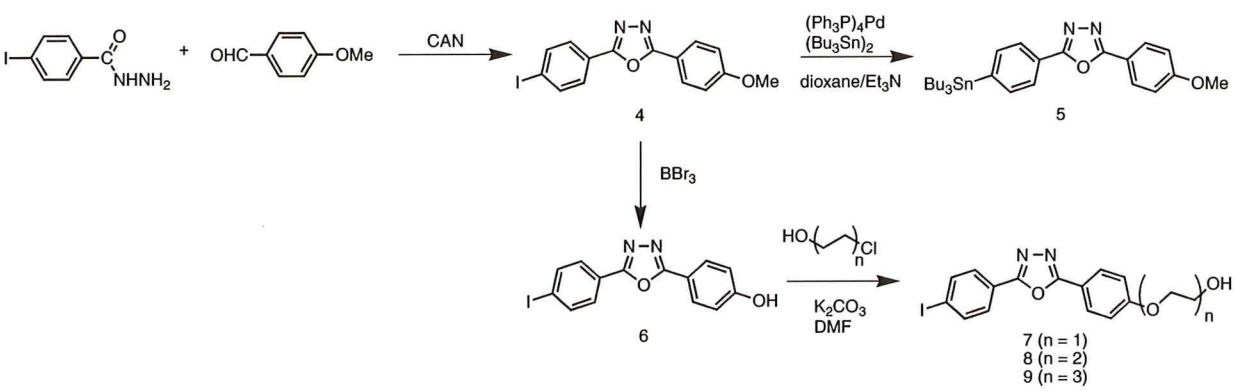

Scheme 2.

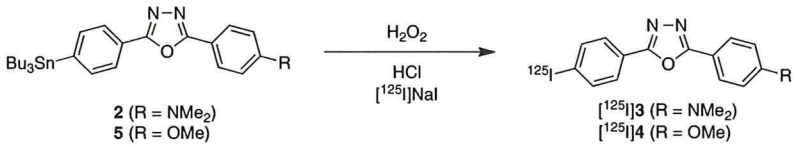

Scheme 3.

Table 1
Inhibition constants (K_i) for binding of 1,3,4-DPOD derivatives determined using [^{125}I]IMPY as the ligand in Aβ42 aggregates

Compound	K_i[a] (nM)
3	20.1 ± 2.5
4	46.1 ± 12.6
6	229.6 ± 47.3
7	282.2 ± 61.4
8	348.6 ± 51.7
9	257.7 ± 34.8

[a] Values are the mean ± standard error for the mean for 4–6 independent experiments.

Table 2
Partition coefficients for 1,2,4-DPOD and 1,3,4-DPOD derivatives

Compound	Log P[a]
3	2.43 ± 0.07
4	2.58 ± 0.06
1,2,4-DPOD-DM	3.22 ± 0.01
1,2,4-DPOD-OMe	3.37 ± 0.04

[a] Octanol/buffer (0.1 M phosphate-buffered saline, pH 7.4) partition coefficients. Each value represents the mean ± SD for 2–3 experiments.

Table 3
Biodistribution of radioactivity after injection of [^{125}I]1,3,4-DPOD derivatives in normal mice[a]

Tissue	Time after injection (min)			
	2	10	30	60
[^{125}I]**3**				
Blood	3.28 (0.46)	3.51 (0.29)	2.53 (0.28)	2.21 (0.41)
Liver	15.87 (3.49)	19.12 (2.43)	12.64 (2.44)	10.01 (1.64)
Kidney	9.14 (1.60)	7.80 (0.64)	5.71 (1.35)	3.81 (0.64)
Intestine	2.28 (0.55)	11.34 (1.61)	12.58 (2.35)	16.22 (2.51)
Spleen	3.56 (0.96)	4.10 (0.40)	2.63 (0.54)	2.05 (0.41)
Pancreas	5.32 (0.98)	4.39 (2.17)	2.50 (0.56)	2.14 (0.90)
Heart	3.99 (3.10)	3.55 (1.86)	2.03 (0.30)	1.54 (0.31)
Stomach[b]	1.40 (0.10)	4.73 (1.86)	4.79 (1.12)	5.50 (0.51)
Brain	2.98 (0.53)	5.93 (0.76)	3.16 (0.69)	1.78 (0.41)
[^{125}I]**4**				
Blood	1.84 (0.30)	1.60 (0.30)	1.26 (0.26)	0.80 (0.20)
Liver	9.60 (1.73)	12.60 (1.14)	8.07 (1.66)	4.65 (1.34)
Kidney	7.14 (1.46)	4.85 (0.48)	4.36 (1.12)	2.48 (0.37)
Intestine	2.07 (0.36)	4.49 (0.60)	10.06 (1.81)	19.85 (4.71)
Spleen	2.44 (0.28)	1.51 (0.26)	0.80 (0.10)	0.60 (0.26)
Pancreas	4.74 (0.63)	1.98 (0.37)	0.96 (0.03)	0.57 (0.14)
Heart	4.80 (1.33)	1.73 (0.27)	0.92 (0.25)	0.43 (0.11)
Stomach[b]	0.71 (0.13)	1.41 (0.91)	3.12 (0.90)	2.90 (1.57)
Brain	3.75 (0.78)	2.74 (0.37)	1.04 (0.14)	0.36 (0.13)

[a] Expressed as % injection dose per gram. Each value represents the mean (SD) for 4–6 animals.
[b] Expressed as % injected dose per organ.

the ideal Aβ-imaging agent should have good brain penetration to deliver the intended dose into the brain, while maintaining a fast washout from normal tissues. Because the normal brain has no Aβ plaques to trap the agent, the washout from the brain should also be fast. Once the high affinity ligand is delivered into the regions containing the Aβ plaques, imaging agents such as [^{125}I]**3** and [^{125}I]**4** are expected to be trapped in this region longer due to its high binding affinity. The differences between the kinetics in normal and Aβ plaque-containing regions will result in a higher signal to noise ratio (target to non-target ratio) in the AD brain. Based on the data presented for [^{125}I]1,3,4-DPOD, it is predicted that the brain trapping of [^{125}I]1,3,4-DPOD in Aβ-containing regions will be much better than that of [^{125}I]1,2,4-DPOD. The log P values of 1,3,4-DPOD derivatives (log P = 2.43 and 2.58 for **3** and **4**, respectively) were lower than those of 1,2,4-DPOD derivatives (log P = 3.22 and 3.37 for 1,2,4-DPOD-DM and 1,2,4-DPOD-OMe, respectively). Although many factors such as molecular size, ionic charge, and lipophilicity affect the uptake of a compound into the brain, the difference in lipophilicity may be one reason for the difference in brain uptake and washout between 1,3,4-DPOD and 1,2,4-DPOD. Further structural modifications, that is, decreasing the lipophilicity by introducing the hydrophilic group, should improve the in vivo properties of 1,3,4-DPOD derivatives.

3. Conclusion

In conclusion, we successfully designed and synthesized a new series of 1,3,4-DPOD derivatives as probes for the in vivo imaging of Aβ plaques in the brain. In in vitro binding experiments, these 1,3,4-DPOD derivatives showed affinity for Aβ42 aggregates. The 1,3,4-DPOD derivatives clearly stained Aβ plaques in an animal model of AD, reflecting their affinity for Aβ aggregates in vitro. Compared to 1,2,4-DPOD, they displayed good penetration of and a fast washout from the brain in biodistribution experiments using

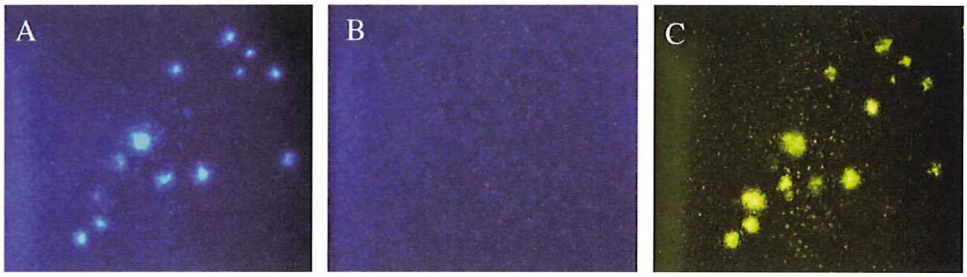

Figure 2. Neuropathological staining of compound **3** on 10-μm AD model mouse sections (A) and wild-type mouse sections (B). Labeled plaques were confirmed by staining of the adjacent sections with thioflavin S (C).

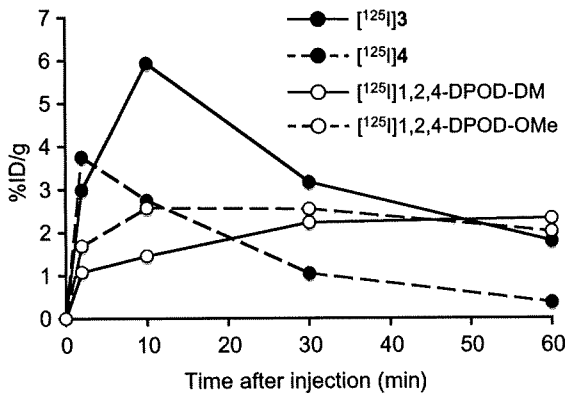

Figure 3. Comparison of brain uptake of [^{125}I]**3**, [^{125}I]**4**, [^{125}I]1,2,4-DPOD-DM and [^{125}I]1,2,4-DPOD-OMe in normal mice. The kinetics of the uptake of [^{125}I]**3** and [^{125}I]**4** may provide a better pattern for the localization of Aβ plaques in the brain.

normal mice. Taken together, the present results suggested that the novel radioiodinated 1,3,4-DPOD derivatives may be useful probes for detecting Aβ plaques in the AD brain.

4. Experimental

4.1. General

All reagents were commercial products and used without further purification unless otherwise indicated. ^{1}H NMR spectra were obtained on a Varian Gemini 300 spectrometer with TMS as an internal standard. Coupling constants are reported in hertz. Multiplicity is defined by s (singlet), d (doublet), t (triplet), and m (multiplet). ^{13}C NMR spectra were obtained on an AL400 JEOL spectrometer with TMS as an internal standard. Mass spectra were obtained on a JEOL IMS-DX.

4.1.1. 4-(5-(4-Bromophenyl)-1,3,4-oxadiazol-2-yl)-*N*,*N*-dimethylbenzenamine (1)

To a solution of 4-bromobenzhydrazide (215 mg, 1 mmol) and 4-dimethylaminobenzaldehyde (149 mg, 1 mmol) in dry CH_2Cl_2 (10 mL) was added CAN (548 mg, 1 mmol). The reaction mixture was stirred under reflux for 24 h. Water was added and following extraction with $CHCl_3$, the organic phase was dried over Na_2SO_4. The solvent was removed and the residue was purified by silica gel chromatography (hexane/ethyl acetate = 4:1) to give 12 mg of **1** (3.5%). ^{1}H NMR (300 MHz, $CDCl_3$) δ 3.08 (s, 6H), 6.76 (d, J = 9.0 Hz, 2H), 7.66 (d, J = 8.4 Hz, 2H), 7.98 (dd, J = 5.4, 4.5 Hz, 4H). MS m/z 362 (M^+).

4.1.2. 4-(5-(4-Tributylstannyl)phenyl)-1,3,4-oxadiazol-2-yl)-*N*,*N*-dimethylbenzenamine (2)

A mixture of **1** (19 mg, 0.06 mmol), bis(tributyltin) (0.04 mL) and $(Ph_3P)_4Pd$ (3 mg, 0.002 mmol) in a mixed solvent (6 mL, 1:1 dioxane/Et_3N) was stirred under reflux for 4.5 h. The solvent was removed, and the residue was purified by silica gel chromatography (hexane/ethyl acetate = 3:1) to give 2.5 mg of **2** (8.2%). ^{1}H NMR (300 MHz, $CDCl_3$) δ 0.87–1.6 (m, 27H), 3.07 (s, 6H), 6.77 (d, J = 9.0 Hz, 2H), 7.61 (d, J = 8.4 Hz, 2H), 8.01 (dd, J = 9.0, 8.1 Hz, 4H).

4.1.3. 4-(5-(Iodophenyl)-1,3,4-oxadiazol-2-yl)-*N*,*N*-dimethylbenzenamine (3)

The same reaction as described above to prepare **1** was used, and 14 mg of **3** was obtained in a 1.8% yield from 4-iodobenzohydrazide and 4-dimethylaminobenzaldehyde. ^{1}H NMR (300 MHz, $CDCl_3$) δ 3.07 (s, 6H), 6.76 (d, J = 3.0 Hz, 2H), 7.85 (d, J = 12.0 Hz, 4H), 7.97 (d, J = 3.0 Hz, 2H). ^{13}C NMR (400 MHz, $CDCl_3$) δ 40.1, 97.8, 110.7, 111.6, 123.9, 128.0, 128.4, 138.2, 152.5, 162.9, 165.5. HRMS m/z $C_{16}H_{14}N_3OI$ found 391.0191/ calcd 391.0182 (M^+).

4.1.4. 2-(4-Iodophenyl)-5-(4-methoxyphenyl)-1,3,4-oxadiazole (4)

The same reaction as described above to prepare **1** was used, and 40 mg of **4** was obtained in a 8.8% yield from 4-iodobenzohydrazide and 4-methoxybenzaldehyde. ^{1}H NMR (300 MHz, $CDCl_3$) δ 3.89 (s, 3H), 7.03 (d, J = 2.9 Hz, 2H), 7.86 (q, J = 7.8 Hz, 4H), 8.03 (d, J = 3.0 Hz, 2H). ^{13}C NMR (400 MHz, $CDCl_3$) δ 55.5, 98.2, 114.6, 116.2, 123.6, 128.1, 128.8, 138.3, 162.5, 163.6, 164.7. HRMS m/z $C_{15}H_{11}N_2O_2I$ found 377.9877, calcd 377.9865 (M^+).

4.1.5. 2-(4-(Tributylstannyl)phenyl)-5-(4-methoxyphenyl)-1,3,4-oxadiazole (5)

The same reaction as described above to prepare **2** was used, and 6 mg of **5** was obtained in a 6.5% yield from **4**. ^{1}H NMR (300 MHz, $CDCl_3$) δ 0.87–1.58 (m, 27H), 3.91 (s, 3H), 7.04 (d, J = 3.1 Hz, 2H), 7.63 (d, J = 2.6 Hz, 2H), 8.06 (q, J = 6.6 Hz, 4H).

4.1.6. 4-(5-(4-Iodophenyl)-1,3,4-oxadiazol-2-yl)phenol (6)

BBr_3 (0.6 mL, 1 M solution in CH_2Cl_2) was added to a solution of **4** (36 mg, 0.1 mmol) in CH_2Cl_2 (16 mL) dropwise in an ice bath. The mixture was allowed to warm to room temperature and stirred for 5 days. Water (50 mL) was added while the reaction mixture was cooled in an ice bath. The mixture was extracted with $CHCl_3$ (30 mL) and the water layer was extracted with ethyl acetate. The organic phase was dried over Na_2SO_4 and filtered. The solvent was removed, and the residue was purified by silica gel chromatography (hexane/ethyl acetate = 2:1) to give 17 mg of **6** (49.0%). ^{1}H NMR (300 MHz, $CDCl_3$) δ 6.98–7.06 (m, 2H), 7.86–7.91 (m, 4H), 8.02–8.09 (m, 2H). HRMS m/z $C_{14}H_9N_2O_2I$ found 363.9712, calcd 363.9709 (M^+).

4.1.7. 2-(4-(5-(4-Iodophenyl)-1,3,4-oxadiazol-2-yl)phenoxy)ethanol (7)

A mixture of **6** (22 mg, 0.06 mmol), potassium carbonate (24.5 mg, 0.18 mmol) and ethylene chlorohydrin (4 μL, 0.06 mmol) in anhydrous DMF (3 mL) was stirred under reflux for 6.5 h. After cooling to room temperature, water was added, and the reaction mixture was extracted with $CHCl_3$. The organic layer was separated, dried over Na_2SO_4 and evaporated. The resulting residue was purified by silica gel chromatography (hexane/ethyl acetate = 2:3) to give 11 mg of **7** (44.6%). ^{1}H NMR (300 MHz, $CDCl_3$) δ 4.03 (q, J = 5.0 Hz, 2H), 4.18 (d, J = 3.0 Hz, 2H) 7.06 (d, J = 3.0 Hz, 2H), 7.87 (q, J = 8.0 Hz, 4H), 8.07 (d, J = 3.0 Hz, 2H). HRMS m/z $C_{16}H_{13}N_2O_3I$ found 407.9983, calcd 407.9971 (M^+).

4.1.8. 2-(2-(4-(5-(4-Iodophenyl)-1,3,4-oxadiazol-2-yl)phenoxy)ethoxy)ethanol (8)

The same reaction as described above to prepare **7** was used, and 9 mg of **8** was obtained in a 25.9% yield from **6** and ethylene glycol mono-2-chloroethyl ether. ^{1}H NMR (300 MHz, $CDCl_3$) δ 3.70 (t, J = 3.1 Hz, 2H), 3.79 (q, J = 4.8 Hz, 2H), 3.92 (t, J = 3.2 Hz, 2H), 4.23 (t, J = 3.1 Hz, 2H), 7.06 (d, J = 3.1 Hz, 2H), 7.87 (q, J = 7.6 Hz, 4H), 8.70 (d, J = 3.1 Hz, 2H). HRMS m/z $C_{18}H_{17}N_2O_4I$ found 452.0244, calcd 452.0233 (M^+).

4.1.9. 2-(2-(2-(4-(5-(4-Iodophenyl)-1,3,4-oxadiazol-2-yl)phenoxy)ethoxy)ethoxy)ethanol (9)

The same reaction as described above to prepare **7** was used, and 7.8 mg of **9** was obtained in a 44.7% yield from **6** and 2-[2-(chloroethoxy)ethoxy]ethanol. ^{1}H NMR (300 MHz, $CDCl_3$) δ 3.61–3.77 (m, 8H), 3.91 (t, J = 3.1 Hz), 4.23 (t, J = 3.2 Hz, 2H), 7.06 (d,

J = 3.0 Hz, 2H), 7.87 (q, J = 7.8 Hz, 4H), 8.06 (d, J = 2.3 Hz, 2H). HRMS m/z $C_{20}H_{21}N_2O_5I$ found 496.0525, calcd 496.0495 (M^+).

4.2. Iododestannylation reaction

The radioiodinated forms of compounds **3** and **4** were prepared from the corresponding tributyltin derivatives by iododestannylation. Briefly, to initiate the reaction, 50 μL of H_2O_2 (3%) was added to a mixture of a tributyltin derivative (50 μg/50 μL EtOH), [^{125}I]NaI (0.1–0.2 mCi, specific activity 2200 Ci/mmol), and 50 μL of 1 N HCl in a sealed vial. The reaction was allowed to proceed at room temperature for 3 min and terminated by addition of $NaHSO_3$. After neutralization with sodium biocarbonate and extraction with ethyl acetate, the extract was dried by passing through an anhydrous Na_2SO_4 column and then blown dry with a stream of nitrogen gas. The radioiodinated ligand was purified by HPLC on a Cosmosil C_{18} column with an isocratic solvent of H_2O/acetonitrile (4:6) at a flow rate of 1.0 mL/min.

4.3. Binding assays using the aggregated Aβ peptide in solution

A solid form of Aβ42 was purchased from Peptide Institute (Osaka, Japan). Aggregation was carried out by gently dissolving the peptide (0.25 mg/mL) in a buffer solution (pH 7.4) containing 10 mM sodium phosphate and 1 mM EDTA. The solution was incubated at 37 °C for 42 h with gentle and constant shaking. Binding assays were carried out as described previously.[24] [^{125}I]IMPY (6-iodo-2-(4'-dimethylamino)phenyl-imidazo[1,2]pyridine) with 2200 Ci/mmol specific activity and greater than 95% radiochemical purity was prepared using the standard iododestannylation reaction as described previously.[15] Binding assays were carried out in 12 × 75 mm borosilicate glass tubes. A mixture containing 50 μL of test compound (0.2 pM–400 μM in 10% EtOH), 50 μL of [^{125}I]IMPY (0.02 nM diluted in 10%EtOH), 50 μL of Aβ42 aggregates, and 850 μL of 10% ethanol was incubated at room temperature for 3 h. The mixture was then filtered through Whatman GF/B filters using a Brandel M-24 cell harvester, and the filters containing the bound ^{125}I ligand were placed in a gamma counter (Aloka, ARC-380). Values for the half-maximal inhibitory concentration (IC_{50}) were determined from displacement curves of three independent experiments using GraphPad Prism 4.0, and those for the inhibition constant (K_i) were calculated using the Cheng–Prusoff equation.[25]

4.4. Neuropathological staining of model mouse brain sections

The experiments with animals were conducted in accordance with our institutional guidelines and were approved by Nagasaki University Animal Care Committee. The Tg2576 transgenic mice (female, 28-month-old) and wild-type mice (female, 28-month-old) were used as the Alzheimer's model and control mice, respectively. After the mice were sacrificed by decapitation, the brains were immediately removed and frozen in powdered dry ice. The frozen blocks were sliced into serial sections, 10 μm thick. Each slide was incubated with a 50% EtOH solution (100 μM) of compounds **3** and **4** for 30 min. The sections were washed in 50% EtOH for 1 min two times, and examined using a microscope (Nikon Eclipse 80i) equipped with a UV-1A filter set (excitation, 365–375 nm; diachronic mirror, 400 nm; longpass filter, 400 nm). Thereafter, the serial sections were also stained with thioflavin S, a pathological dye commonly used for staining Aβ plaques in the brain, and examined using a microscope (Nikon Eclipse 80i) equipped with a B-2A filter set (excitation, 450–480 nm; diachronic mirror, 505 nm; longpass filter, 520 nm).

4.5. Determination of partition coefficient determination

Partition coefficients were measured by mixing [^{125}I]**3** and [^{125}I]**4** with 1.5 mL each of 1-octanol and buffer (0.1 M phosphate, pH 7.4) in a test tube. The test tube was vortexed for 20 s three times. Two weighed samples (1 mL each) from the 1-octanol and buffer layers were measured for radioactivity with a gamma counter. The partition coefficient was determined by calculating the ratio of cpm/1 mL of 1-octanol to that of the buffer.

4.6. In vivo biodistribution in normal mice

A saline solution (100 μL) of radiolabeled agents (0.2–0.4 μCi) containing ethanol (10 μL) was injected intravenously directly into the tail of ddY mice (5-week-old, 22–25 g). The mice were sacrificed at various time points postinjection. The organs of interest were removed and weighed, and radioactivity was measured with an automatic gamma counter (Aloka, ARC-380).

Acknowledgments

This study was supported by the Program for Promotion of Fundamental Studies in Health Sciences of the National Institute of Biomedical Innovation (NIBIO) and a Health Labour Sciences Research Grant.

References and notes

1. Klunk, W. E. *Neurobiol. Aging* **1998**, *19*, 145.
2. Hardy, J.; Selkoe, D. J. *Science* **2002**, *297*, 353.
3. Mathis, C. A.; Lopresti, B. J.; Klunk, W. E. *Nucl. Med. Biol.* **2007**, *34*, 809.
4. Mathis, C. A.; Wang, Y.; Klunk, W. E. *Curr. Pharm. Des.* **2004**, *10*, 1469.
5. Nordberg, A. *Lancet Neurol.* **2004**, *3*, 519.
6. Mathis, C. A.; Wang, Y.; Holt, D. P.; Huang, G. F.; Debnath, M. L.; Klunk, W. E. *J. Med. Chem.* **2003**, *46*, 2740.
7. Klunk, W. E.; Engler, H.; Nordberg, A.; Wang, Y.; Blomqvist, G.; Holt, D. P.; Bergstrom, M.; Savitcheva, I.; Huang, G. F.; Estrada, S.; Ausen, B.; Debnath, M. L.; Barletta, J.; Price, J. C.; Sandell, J.; Lopresti, B. J.; Wall, A.; Koivisto, P.; Antoni, G.; Mathis, C. A.; Langstrom, B. *Ann. Neurol.* **2004**, *55*, 306.
8. Ono, M.; Wilson, A.; Norbrega, J.; Westaway, D.; Verhoeff, P.; Zhuang, Z. P.; Kung, M. P.; Kung, H. F. *Nucl. Med. Biol.* **2003**, *30*, 565.
9. Verhoeff, N. P.; Wilson, A. A.; Takeshita, S.; Trop, L.; Hussey, D.; Singh, K.; Kung, H. F.; Kung, M. P.; Houle, S. *Am. J. Geriatr. Psychiatry* **2004**, *12*, 584.
10. Rowe, C. C.; Ackerman, U.; Browne, W.; Mulligan, R.; Pike, K. L.; O'Keefe, G.; Tochon-Danguy, H.; Chan, G.; Berlangieri, S. U.; Jones, G.; Dickinson-Rowe, K. L.; Kung, H. P.; Zhang, W.; Kung, M. P.; Skovronsky, D.; Dyrks, T.; Holl, G.; Krause, S.; Friebe, M.; Lehman, L.; Lindemann, S.; Dinkelborg, L. M.; Masters, C. L.; Villemagne, V. L. *Lancet Neurol.* **2008**, *7*, 129.
11. Kudo, Y.; Okamura, N.; Furumoto, S.; Tashiro, M.; Furukawa, K.; Maruyama, M.; Itoh, M.; Iwata, R.; Yanai, K.; Arai, H. *J. Nucl. Med.* **2007**, *48*, 553.
12. Agdeppa, E. D.; Kepe, V.; Liu, J.; Flores-Torres, S.; Satyamurthy, N.; Petric, A.; Cole, G. M.; Small, C. W.; Huang, S. C.; Barrio, J. R. *J. Neurosci.* **2001**, *21*, RC189.
13. Shoghi-Jadid, K.; Small, G. W.; Agdeppa, E. D.; Kepe, V.; Ercoli, L. M.; Siddarth, P.; Read, S.; Satyamurthy, N.; Petric, A.; Huang, S. C.; Barrio, J. R. *Am. J. Geriatr. Psychiatry* **2002**, *10*, 24.
14. Small, G. W.; Kepe, V.; Ercoli, L. M.; Siddarth, P.; Bookheimer, S. Y.; Miller, K. J.; Lavretsky, H.; Burggren, A. C.; Cole, G. M.; Vinters, H. V.; Thompson, P. M.; Huang, S. C.; Satyamurthy, N.; Phelps, M. E.; Barrio, J. R. *N. Engl. J. Med.* **2006**, *355*, 2652.
15. Kung, M. P.; Hou, C.; Zhuang, Z. P.; Zhang, B.; Skovronsky, D.; Trojanowski, J. Q.; Lee, V. M.; Kung, H. F. *Brain Res.* **2002**, *956*, 202.
16. Zhuang, Z. P.; Kung, M. P.; Wilson, A.; Lee, C. W.; Plossl, K.; Hou, C.; Holtzman, D. M.; Kung, H. F. *J. Med. Chem.* **2003**, *46*, 237.
17. Newberg, A. B.; Wintering, N. A.; Plossl, K.; Hochold, J.; Stabin, M. G.; Watson, M.; Skovronsky, D.; Clark, C. M.; Kung, M. P.; Kung, H. F. *J. Nucl. Med.* **2006**, *47*, 748.
18. Newberg, A. B.; Wintering, N. A.; Clark, C. M.; Plossl, K.; Skovronsky, D.; Seibyl, J. P.; Kung, M. P.; Kung, H. F. *J. Nucl. Med.* **2006**, *47*, 78.
19. Ono, M.; Haratake, M.; Saji, H.; Nakayama, M. *Bioorg. Med. Chem.* **2008**, *16*, 6867.
20. Neaterov, E. E.; Skoch, J.; Hyman, B. T.; Klunk, W. E.; Bacskai, B. J.; Swager, T. M. *Angew. Chem. Int. Ed.* **2005**, *44*, 5452.
21. Chabdra, R.; Kung, M. P.; Kung, H. F. *Bioorg. Med. Chem. Lett.* **2006**, *16*, 1350.
22. Qu, W.; Kung, M. P.; Hou, C.; Oya, S.; Kung, H. F. *J. Med. Chem.* **2007**, *50*, 3380.
23. Dabiti, M.; Salehi, P.; Baghbanzadeh, M.; Bahramnejad, M. *Tetrahedron Lett.* **2006**, *47*, 6983.
24. Kung, M. P.; Hou, C.; Zhuang, Z. P.; Skovronsky, D.; Kung, H. F. *Brain Res.* **2004**, *1025*, 98.
25. Cheng, Y.; Prusoff, W. H. *Biochem. Pharmacol.* **1973**, *22*, 3099.